공학박사학위논문

Study of Anode Supported GDC/YSZ Bi-layered Electrolyte Solid Oxide Fuel Cell via Cold Press Process

콜드 프레스 공정을 이용한 음극지지체 GDC/YSZ 전해질 이중층 고체산화물 연료전지 연구

2014 년 2 월

서울대학교 대학원

기계항공공학부

최 훈

Study of Anode Supported GDC/YSZ Bi-layered Electrolyte Solid Oxide Fuel Cell via Cold Press Process

By

Hoon Choi

Submitted in Partial Fulfillment of the Requirements for the Degree of Doctor of Philosophy

Department of Mechanical and Aerospace Engineering
Seoul National University

February 2014

Abstract

The fact that hydrogen will be the last energy source became no more attractive to us. The main issue is which kind of energy conversion device will be going to survive in the future. Since many researchers highlighted the fuel cell as the next generation power source, a lot of researched have been conducted to commercialize it.

SOFCs have many advantages in comparison with typical PEMFCs which have shown water management problem, usage of novel catalyst, patent issue for polymer electrolyte, expansive graphite bipolar plate and CO poisoning. So many researchers in energy field have been thought SOFC would be the promising device.

But the main bottle neck for the commercialization of SOFC has been its high operation temperature. It can cause thermal mismatch between MEA, nickel agglomeration, reactions between component materials, restricted sealant choice and expensive interconnecter material. So we focused our interest to IT-SOFC. Its temperature position can avoid many problems of HTSOFC and LT-SOFC maintaining the competitiveness of original SOFC's characteristics. Moreover, process cost issue about compaction, sintering and more complicated high temperature process is one of the bottle-neck for commercialization.

In this study, we studied the lower the operating temperature in order to solve these problems, while reducing the thickness of the electrolyte and dropping the number of steps compared to the conventional method.

First, we prepared the bi-layer electrolyte solid oxide fuel cell which was deposited yttria-stabilized zirconia (YSZ) and gadolinia dopted ceria (GDC) which

is high ionic conductivity material at low and intermediate temperature. This structure is verified that high performance, sufficient durability and operation in a low temperature.

It is confirmed the successful deposition of YSZ through the scanning electron microscope (SEM) and X-ray photoelectron spectroscopy (XPS). We obtained a 50% improvement power density and 5% higher open circuit voltage (OCV) than the output of pure GDC electrolyte cell at 600 degrees Celsius. We confirmed that the YSZ layer prevent enhancing electronic conductivity and micro crack which can make voltage-drop and enlarge ohmic loss in order to reduce GDC layer by SEM image and EIS.

Second, because we verified effect of YSZ/GDC bi-layer electrolyte structure to the performance, it is studied about bi-layer electrolyte anode supported type solid oxide fuel cell structure which could have higher power density. Various wet ceramic processes and thin film deposition processes are employed to electrolyte deposition method to calcined anode substrate. Finally, we established cold press process that can sinter from substrate to electrolyte at one step process.

In order to enhance the controllability and uniformity of thickness of the layer, spray dry coating method that can control about micron range using powder vehicle is employed. The compressed dry powder substrate-bi-layer electrolyte was co-sintered, and we fabricated LSCF-GDC cathode using screen printing method. It is possible as compared with the wet method, to reduce the sintering step one or more times, forming method such a great advantage in time and cost.

We obtained power density of 210mW/cm2 at 600 degrees Celsius, and 409mW/cm2 at 800 degrees Celsius from prepared bi-layer electrolyte cell. It is

0.1V higher open circuit voltage and 15% higher maximum power density rather than one of non bi-layer electrolyte cell.

Third, we have improved the fabrication process to increase the performance of bi-layer electrolyte cell via cold press process. In order to make porous anode substrate, the PMMA powder was mixed with anode substrate powder which is used previous bi-layer electrolyte cell fabrication. And it is achieved the power density is 460mW/cm2 at 700 degrees Celsius. Further, by adding one functional layer between the anode substrate and electrolyte layer, to complement the reduction in mechanical strength that can occur in the case of porous anode support, to improve the electrochemical performance by cold press process. As a result, it was possible to obtain a power density and mechanical strength is enhanced, and is more stably maintained even during operation.

Finally, we modeled and calculated the compaction behavior during cold press process using COMSOL multiphysics. The Surface von Mise stress was predicted using the Drucker-Prager Cap model. Through this model, we were able to determine at the time of production to minimize the damage, and the condition of the powder. In addition, through the modeling, the basic direction for the production of large-scale cells could be present.

Keywords: solid oxide fuel cell (SOFC), intermediate temperature, gadolinia doped ceria (GDC), bi-layered electrolyte

Identification Number: 2007-20864

Contents

List of figures

List of tables

Chapter 1. Introduction

1.1 Research Background

Nowadays, we could know that oil price would threaten the stability of world energy economy. The fears to reduction of natural resources and the rapid resource consumption from the industrialization have become direct and indirect origins of international conflicts. Energy became a big issue cause of the increase of the demand for portable power due to the spread of mobile individual devices like smartphone, tablet PC or ubiquitous applications.

Moreover, environmental issue is one of the most important agenda in energy industry. Due to the fossil fuel problems, so many discussions have been. Many congresses something like Tokyo protocol proposed to regulate the usage of carbon dioxide (CO2), methane (CH4), nitrogen dioxide (NO2), fluorocarbon (PFC), hydrofluorocarbon (HFC) and sulfur nexafluoride (SF6). Moreover, they encourage the conversion to hydrogen economy for clean energy systems.

In this focus, the future energy paradigm suggested by Department of Energy (DOE) that hydrogen production and the circulation by fuel cells. The fuel cell is a energy conversion application which can change the chemical energy to the electric energy that can be used for us directly. This direct energy conversion system is classified from a conventional internal combustion generator or batteries. In an engine, chemical energy is converted into heat energy, and then heat energy is converted into kinetic energy. Finally kinetic energy is transformed to electric energy. These multi-step conversion procedures were caused lots of energy loss at each step. So the efficiency is dropped down thus more fuel resources must be required. Because an engine is based on fossil fuel combustion, it is inevitable to

create more CO_2 greenhouse gas and pollute the air.

Batteries are one of the nice choices to avoid greenhouse gas and air pollution issues. But they show some disadvantages for example heavy weight, relatively small energy density for long operation, slow recharging, short life due to often charging and discharging cycle and difficult capacity scale up/down. Fuel cells called 3rd generation battery can get continuous fuel supplying that is fuel cell get the liberation from recharging time and space restriction. For a portable application, it means changing fuel cartridges that have much more capacity than batteries. For an electric vehicle application, it means more distance per fueling and more fuel efficiency from light weight.

Many types of fuel cells have be researched and developed since introduced by William Grove first in 1839 in England. The first fuel cell had the simple platinum electrodes structure reacting hydrogen and oxygen each. Figure 1.1 is the operation principal of general fuel cell. Hydrogen gas fed to anode divided to proton ions and electrons. Electrons flow through circuit and load then arrive to cathode. Protons flow through electrolyte which was intended to conduct ion only. Protons and electrons meet oxygen in the air at cathode. Producing water, reaction cycle is finished. The reaction equation is shown below.

$$H_2 + \frac{1}{2}O_2 \rightarrow 2H_2O$$

$$Anode : H_2 \rightarrow 2H^+ + 2e^-$$

$$Cathode : 2H^+ + 2e^- + \frac{1}{2}O_2 \rightarrow 2H_2O \quad (1.1)$$

Fuel cells have three kinds of loss, activation loss, ohmic loss and mass transport loss. These losses expressed heat dissipation, can vary operation condition (current output, feed gas rate, temperature and etc.) and affect the efficiency of the fuel cell. [2]

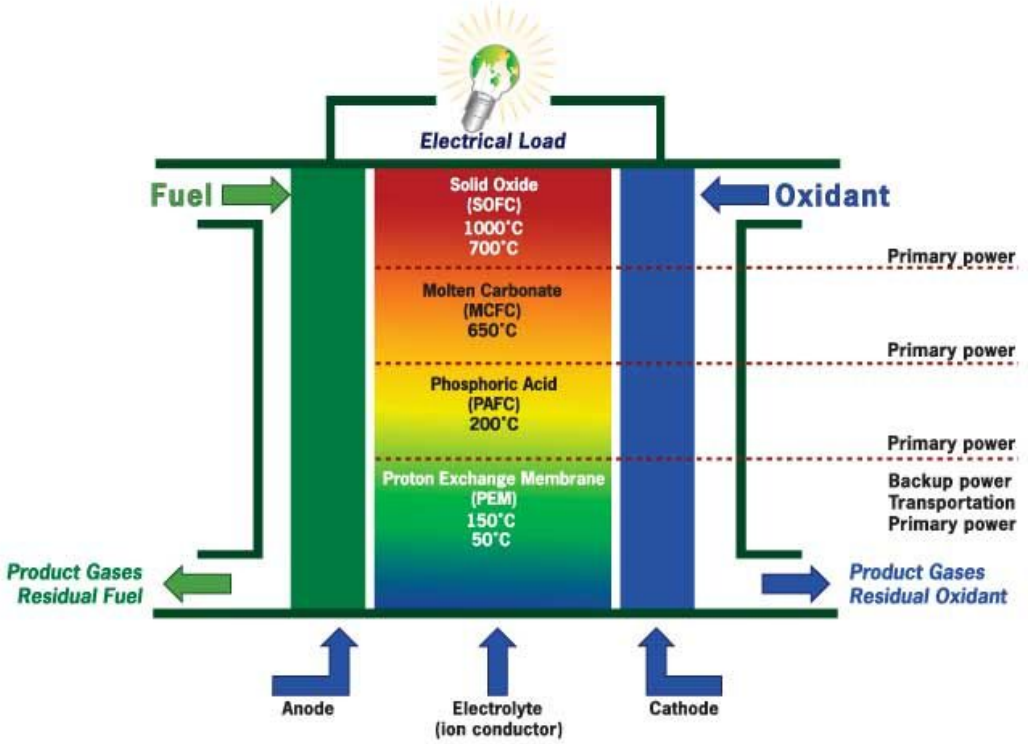

Figure 1.1 Operation principle of a fuel cell [1]

1.2 Solid oxide fuel cell

Many kinds of fuel cells are distinguished according to the electrolyte material, type of reactant (moving ion) and operating temperature. Shown in Table 1.1, many kinds of fuel cells are researched but the studies on PEMFC, DMFC, MCFC and SOFC are more active than others in comparisons of the performance and the possibility of commercialization. AFC and PAFC are studied a lot past time, but nowadays, there are few researches is undergoing. In this study, we focused in solid oxide fuel cell.

SOFC (solid oxide fuel cell) is a fuel cell using ceramic electrolyte conducting oxygen ion in the temperature of 800~1000°C. The representative electrolyte material is yttria stabilized zirconia (YSZ). In a SOFC, water is produced at the anode, rather than at the cathode as in a PEMFC. A schematic diagram of a SOFC is provided in Figure 1.2. The anode is a cermet of nickel and electrolyte material. The cathode is usually a mixed ion-conducting and electronically-conducting ceramic material. Typical cathode materials include strontium-doped lanthanum manganite (LSM), lanthanum strontium ferrite (LSF), lanthanum strontium cobaltite (LSC), and lanthanum strontium cobaltite ferrite (LSCF).

Although overall reaction is same, the reaction in each electrode is some different from other conventional fuel cells.

$$Anode : H_2 + O^{2-} \rightarrow H_2O + 2e^-$$

$$Cathode : \frac{1}{2}O_2 + 2e^- \rightarrow O^{2-} \qquad (1.2)$$

Shown in upper reactions, water is produced at the anode, rather than at the

cathode.

Unlike PEMFC, it is the advantage that SOFC do not suffer water management problem, but SOFC's high temperature also cause poor stability, low durability, thermal compatibility problem and restrict choice of component materials. [4] SOFC is the most efficient among various fuel cells. At the system scale, it can be used for power generation system due to the possibility to re-use waste heat for household application or for cogeneration plant with highest efficiency. It can operate with direct hydrocarbon so reformer is not essential so we can simplify the system components and get high efficiency, too. SOFC can lower down the material cost. The platinum catalyst and graphite bipolar plates in low temperature fuel cells are not used in SOFC. And non-royalty electrolytes are necessary for this fuel cell. Indeed, scale up/down is easier than any other fuel cell. It means various applications can be applicable from the power source of portable and mobile devices through vehicle application to power plant.

Due to these advantages, SOFC is a promising energy conversion device and it is one of the most dynamic research areas in fuel cell field. So this study deals with the methods of commercialization of SOFC.

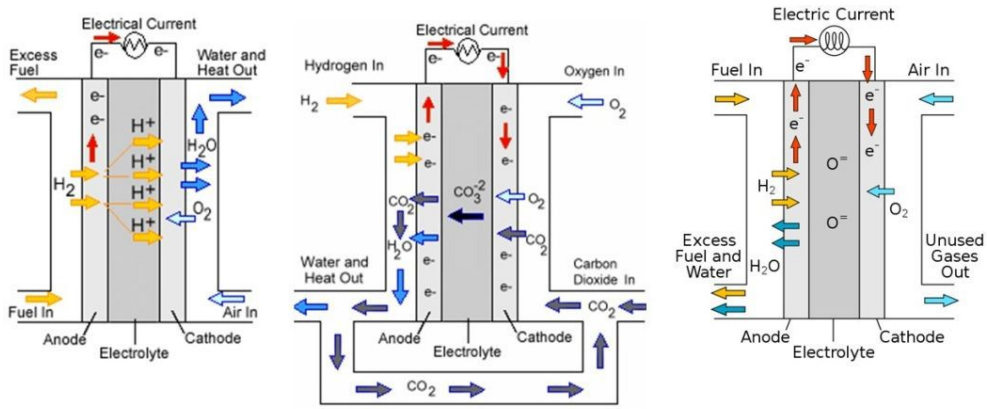

Figure 1.2 Schematics of PEMFC, MCFC and SOFC [5]

Figure 1.3 Advantages of SOFCs

1.3 The operating temperature of SOFCs

Previously written, the typical SOFC has some issues in its high operating temperature. The most significant issue is thermal mismatch between anode electrode and electrolyte or cathode electrode and electrolyte. This means electrodes and electrolyte can be delaminated or broken on elevated temperature to its operating temperature due to the difference of TCE (thermal expansion coefficient) of electrode and electrolyte materials. It has been some problems. First, stability and durability of SOFCs issue is that. Another problem is nickel catalyst agglomeration in anodes. This behavior can disconnect the roots of electron conduction in MIEC (mixed ionic electronic conduction material) and can reduce the TPB (triple phase boundary) area in which the electrochemical reaction occurs so that performance would be drop. Also, the reactions between component materials at the interface in high temperature have been a degradation problem. Some kind of cathode materials like LSCF reacts with ceria based electrolyte in high temperature above 1000°C. Sealing issue is one of the operating temperature issues, too. Above 800°C we cannot use most metal sealant and at about 1000°C using glass based sealant can be restricted. Sealing and separating fuel and air is very important to maintain cell voltage and to prevent component reduction or oxidation. 750°C is the limit temperature for the usage of steel alloy components. Now most of inter-connecter materials are expensive Inconel® and Crofer® that occupy 75% of a SOFC price. A stainless steel based bipolar plate has been a key to cost down a fuel cell system price. So the conventional operating temperature range can be a one of the bottle necks for the commercialization of SOFCs. [6] At the point of view, lots of researches have been focused on lowering the operating temperature.

It can be defined SOFCs into low temperature (LT, ~500°C) SOFC, intermediate temperature (IT, 500°C~800°C) SOFC and high temperature (HT, 800°C~) SOFC. LT-SOFC is most attractive but it is not easy for realizing a large scale cell, finding the proper conductivity electrolyte material, the poor stability Manila, Philippines (MNL-Ninoy Aquino Intl.)problem, using novel metal catalyst. So it is necessary more developed technology now. So we focused our interest to IT-SOFC. Its temperature position can avoid many problems of HT-SOFC and LT-SOFC maintaining the competitiveness of original SOFC's characteristics. Thus we could expect IT-SOFC's high commercialization possibility.

Among the main over potentials of fuel cells; activation loss, ohmic loss and mass transport loss, ohmic over potential is the key of SOFCs performance. It is directly connected to ionic and electronic conductivity of electrolyte. That is, the resistance comes when ions pass through the electrolyte and it is the exactly same idea of resistance in wire which conducts electrons.

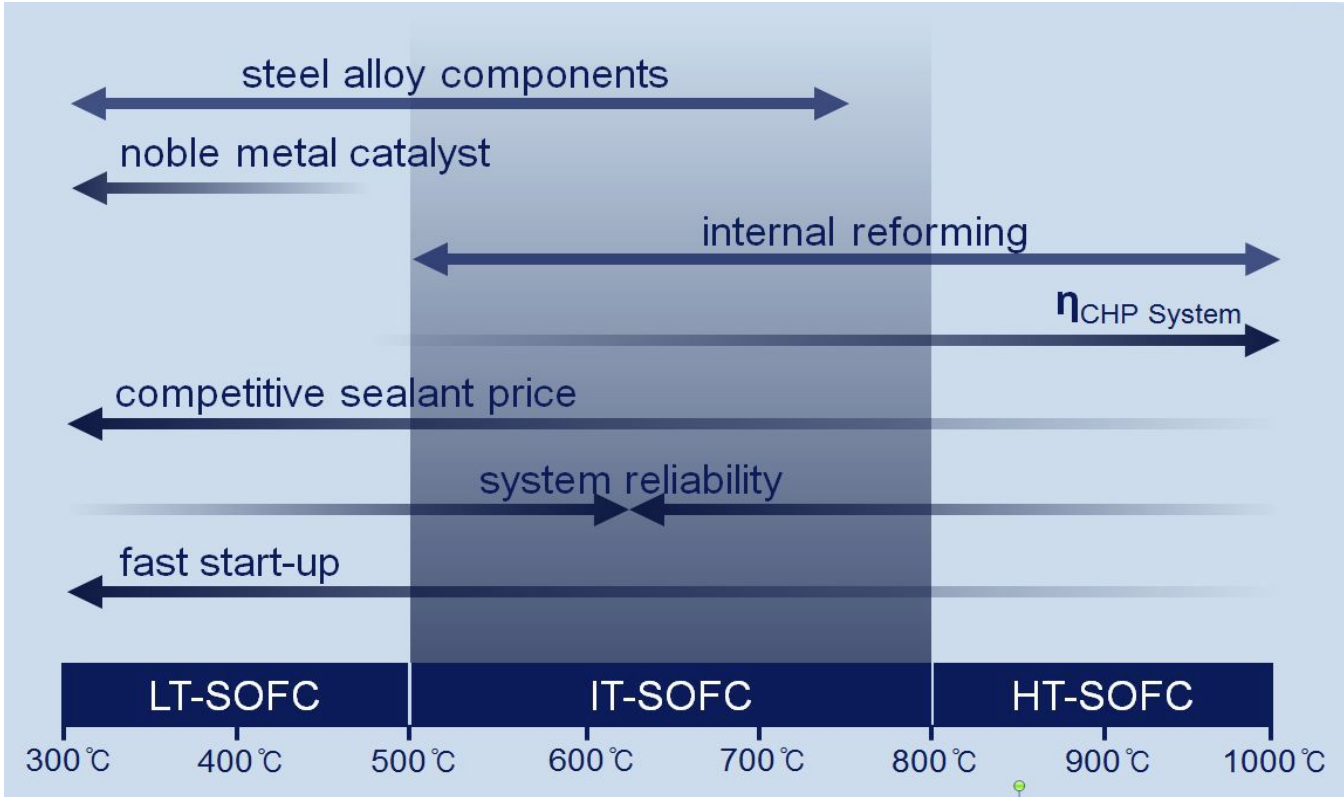

Figure 1.4 Competitiveness of IT-SOFCs

1.3.1 Reducing the thickness of electrolyte

The first method to lower the operation temperature maintaining its performance is reducing the thickness of electrolyte. It means that one makes wire short so that the resistance value is minimized.

$$R = \frac{L}{\sigma(T)} \tag{1.3}$$

In case of SOFC, proper process is required to form a extremely thin, dense and uniform layer which can prevent any gas permeability. Actually typical wet ceramic processes have thickness minimum limit and the possibility of micro pore cannot be ignorable. [7] So the promising technology for reduced thickness electrolyte is thin film deposition technique.

Thin film micro-fabrication methods originally have been used to fabricate semiconductor. To use a typical thin film deposition method, we have to choose adequate one regarding the next conditions. SOFC components have very complex composition where the materials of semiconductor are very simple. If we want to make a porous layer, thin film deposition would not be a good choice. If a substrate which we want to coat with target material is weak, PVD (physical vapor deposition) can be dangerous.

1.3.2 High conductivity electrolytes material

The second method to lower the operation temperature is raised the conductivity of electrolyte. That is, changing the material of wire.

Conventional ZrO_2 based electrolyte materials including YSZ, ScSZ (scandium stabilized zirconia) have wide oxygen partial pressure (PO_2) range, strong mechanical property and chemical stability. But it operates only in high temperature due to poor ionic conductivity.

Bi_2O_3 based materials have 1~2 order higher ionic conductivity than ZrO_2 based. But narrow electrolytic PO_2 range and weak mechanical property, especially reduction into metallic phase Bi below the oxygen partial pressure of 10-13atm at 600°C have been problems to be used for electrolyte. [14]

LSGM electrolyte can be operated in wide PO_2 range with high ionic conductivity. However, if A:B ratio in perovskite structure is off the original point, secondary phase like $LaSrGa_3O_7$, $LaSrGaO_4$ and La_2O_3 can be generated. [14]

CeO_2 based materials including GDC, SDC secure higher ionic conductivity than YSZ. They also have La blocking character from cathode. But in the low PO_2 environment, it shows electron conductivity in the reducing process from Ce^{4+} to Ce^{3+}.

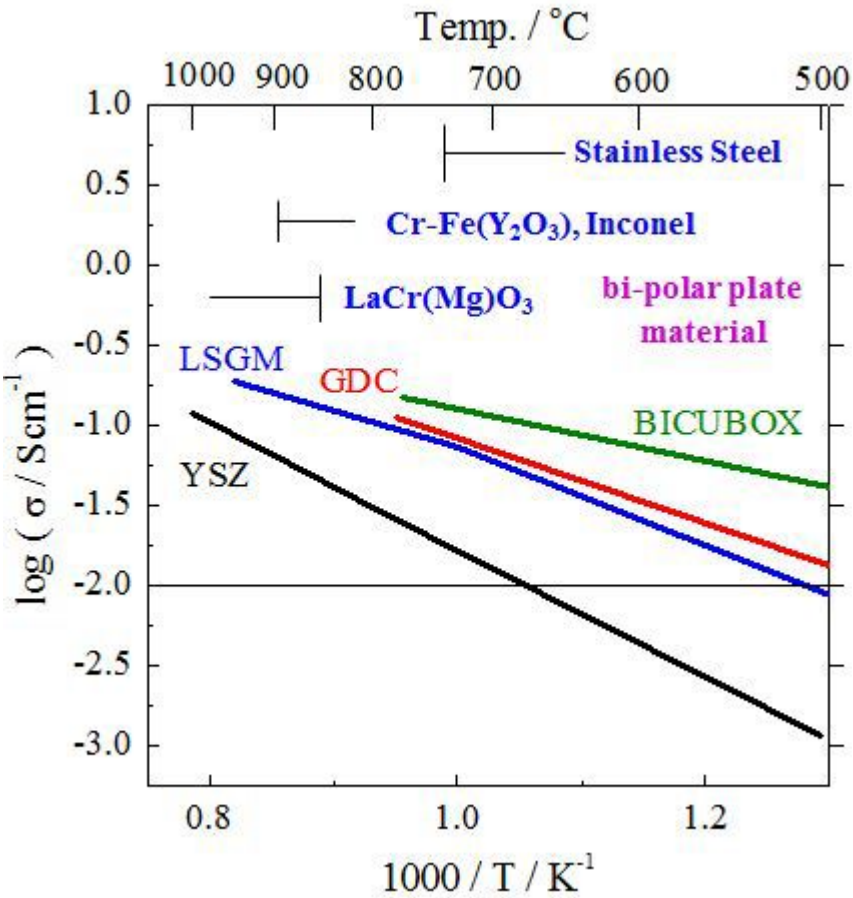

Figure 1.5 Comparison of conductivity of various materials

1.4 Bi-layered electrolytes SOFCs

We decided to fabricate bi-layered electrolyte SOFC for intermediate temperature operation. Base electrolyte material should be high ionic conductive and occupies most electrolyte thickness. And functional electrolyte material should supplement the demerits of main material and be thin. This idea is that combines above two temperature lowering methods.

From 1988 a lot of researchers have been shared bi-layered electrolyte structure technology.

H. Yahiro, Y. Babu, K. Eguchi and H. Arai fabricated YSZ and YDC (yttria doped ceria) bi-layered electrolyte. [15] 1.5μm YSZ was deposited via RF sputtering on 1.5mm YDC. OCV value was 0.82V for pure YDC cell and 0.95V for YSZ/YDC cell at 600°C. At 700°C OCV increased by 0.17V. K. Eguchi and H. Arai made YSZ/SDC bi-layer via RF ion plating. Thickness ratios were 1.86μm/1.825mm and 2μm/1.658mm. At 800°C bi-layered cell showed 0.25V higher OCV. [16],[17]

A. V. Virkar calculated PO2 between bi-layer from a simple equivalent circuit. [18] And he formed YSZ/YDC bi-layer with K. Mehta and R.Xu via spin coating. There were 0.2V OCV increase at 600°C and 0.15V OCV increase at 700°C. [19] R.Xu, K. W. Chour and J. Chen made YSZ/YDC bilayer via MOCVD (metalorganic vapor deposition), EVD+sputtering, sputtering and sol-gel and compared OCV from these methods. EVD+sputtering showed 0.32V OCV increase at 750°C and MOCVD showed 0.27V OCV gap. [20]

Y. Tsai, E. Perry and S. Barnett obtained 0.12V increased OCV with sputtered YSZ/YDC. [21] P. Soral, U. pal and W. L. Worrell made 2μm YSZ and

100μm/10μm GDC bi-layered cell with 0.96V OCV. [22]

An authority on bi-layered electrolyte, E. D. Wachman had interest to ceria and bismuth oxide bi-layered electrolyte. YSB/YDC (yttria doped bismuth oxide) showed 0.08V and 0.04V OCV increases at 700°C and 800°C. ESB/SDC (erbia doped bismuth oxide) showed 0.08V, 0.1V, 0.14V and 0.26 OCV increases at 800°C, 700°C, 600°C and 500°C. [23] With ESB/SDC electrolyte via PLD and spin coating, changing the ESB thickness showed 0.3~0.4V OCV increase. [24] Spray coating 10μm GDC then 4μm ESB on Ni-GDC substrate showed 0.05V more OCV at 650°C. [25]

S. H Chan, X. J. Chen and K. A Khor suggested bi-layered model regarding ion, free electron and electron-hole. [26] S. H Chan, X. J. Chen, K. A Khor and Q. L. Liu measured OCV of the ceramic co-sintered 3μm YSZ and 7μm GDC. The results showed 0.25V, 0.33V and 0.45V increase at 600°C, 700°C and 800°C than 10μm GDC. [27]

Z. Bi, M. Cheng, Y. Dong, H. Wu, Y.She and B. Yi composed 25μm LDC (lanthan doped ceria) / 75μm LSGM electrolyte via dry-pressing. Bilayered cell showed 1.06V OCV where LDC cell showed 0.67V and LSGM showed 1.1V. [28]

R. Maric, D. Ghosh, X. Zhang, M. Robertson, C. Deces-Petit, Y. Xie, R. Hui, S. Yick, E. Styles, J. Roller and O. Kesler made 5μm YSZ / 15μm SDC via co-firing. They obtain 0.22V and 0.38V increased OCV with bi-layered cell at 600°C and 700°C. [29],[30] R. Maric, D. Ghosh, D. Yang, X. Zhang, S. Nikumb, C. Deces-Petit, R. Hui made 1μm ScSZ / 6μm SDC electrolyte cell with 0.2V higher OCV at 600°C. [31] R. Maric, D. Ghosh added the 20μm anode functional layer between anode and bi-layer via spin-coating and result was 0.2V higher OCV. [32]

T. Yamaguchi, S. Shimizu, T. Suzuki, Y. Fujishiro and M. Awano composed ScSZ/GDC via co-sintering and added LSM-GDC layer between cathode and bi-layer. With LSM-GDC layer power density increases were 5.5mW/cm2, 30.5mW/cm2 and 106mW/cm2 at 500°C, 600°C and 700°C.

Younsei university and KIST made GDC substrate via tape-casting (0.44μm) then deposited 2μm YSZ via sol-gel dip drawing with 0.075V, 0.061V and 0.055V OCV increase at 1000°C, 950°C and 900°C. [33] Spincoated 2μm YSZ on 1.6mm YDC showed 0.04V, 0.04V, 0.05V and 0.06V OCV increase at 1000°C, 900°C, 800°C and 700°C. [34]

Table 1.1 Various researches about bi-layer cell process

Type	Process	Thickness	Structure	Temp	OCV	Power den
YSZ/GDC	**screen printing**	3um/5um	Anode/GDC/YSZ/Cathod	600	1.04	
				650	1.03	
				700	1.02	
				750	1.01	
				800	0.99	
YSZ/GDC	**PLD**	-	ni-GDC/GDC/YSZ/LSC	600	0.56	377
		25nm/1mm			1.06	
		50nm/1mm			1.09	1010
		100nm/1mm			1.08	1080
		200nm/1mm			1.09	1140
GDC/YSZ	**RF sputtering**	500nm	Pt-YSZ/YSZ/GDC/Pt-YSZ	400	0.97	1
				450	0.94	125
YSZ/GDC	**RF sputtering**	2um/1mm	Anode/GDC/YSZ/Cathod	600	0.88	
				700	0.8	
				800	0.75	
YSZ/GDC	**dip coating**	5um/45um	Ni-GDC/YSZ/GDC/LSM	650	0.84	520
		45um/5um	Ni-GDC/GDC/YSZ/LSM		1.01	140
YSZ/GDC	**spray coating**	3um/7um	Ni-GDC/YSZ/GDC/LSM-GDC	600	0.86	
					1.107	
				700	0.76	
					1.081	409
				750		570
				800	0.58	
					1.049	678
YSZ/YDC	**sputtering**	1um/8um	Ni-YSZ/YSZ/GDC/LSM-GDC	500	1.089	55
				550	1.068	110
				600	1.03	155
		1.5um/rum	Ni-YSZ/YSZ/YDC/LSM-YSZ		0.88	
		-			1.01	
GDC	**cold press**	15um	Ni-GDC/GDC/SSC	600	0.75	390

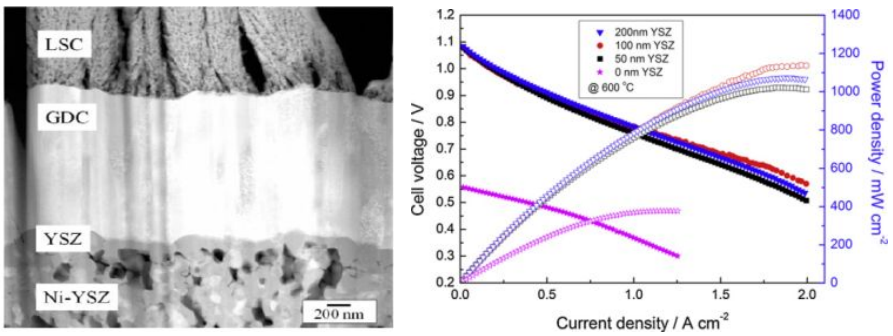

(a) Thin film process(PLD)

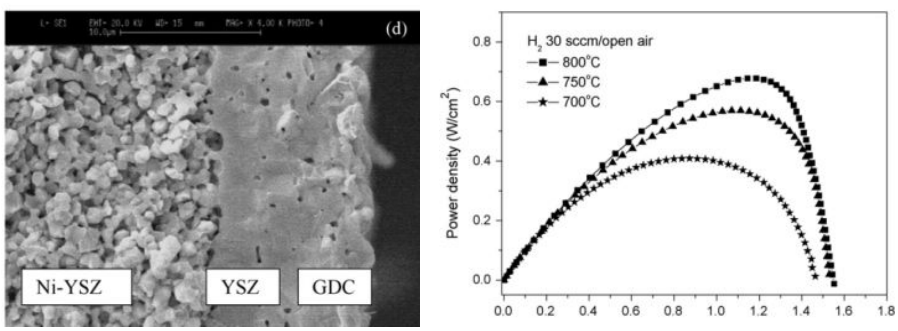

(b) Wet ceramic process (spray coating)

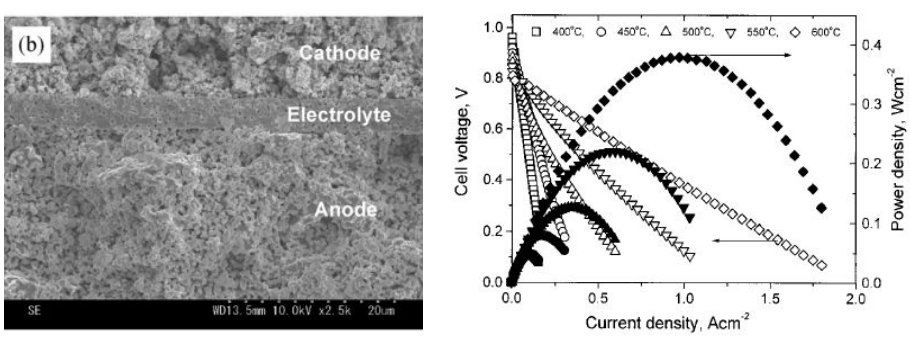

(c) Cold press process (single layer)

Figure 1.6 The various approaches about bi-layer cell fabrication process[23,47,75]

1.5 The supported type of SOFC

The supported type of SOFC is one of the important issues of consist and fabrication cells. The cell of the SOFC consists of ceramic and cermet (ceramic and metallic material). Among anode, electrolyte and cathode, one of the component have to be thick component due to mechanically supported substrate for durability of cell. There are three type of supported cell, cathode supported, electrolyte supported and anode supported SOFC.

The cathode supported cell is employed widely in tubular SOFC cell due to its simple architecture. It has some strong points that low ohmic loss, simple fabrication process and low thermal expansion problems. However, due to thickness of cathode component, it has huge concentration loss and cathodic activation loss. In general, cathode overpotential is much higher than anodic overpotential in SOFC. In high temperature which is operation temperature of SOFCs, hydrogen has high mobility and low activation energy. It leads to low threshold that hydrogen transfer to proton. In the other hands, oxidant in the cathode side has bigger activation energy than hydrogen fuel, so it leads to significant cathodic loss.

The electrolyte supported cell is mostly used supported type. It has many advantages. Electrolyte material is most hard and strength components in SOFC cell components. Yittria stabilized zirconia and doped ceria oxides are one of them. These materials can endure mechanical load and tensile stress rather than anode material or cathode material, so we can make it thinner than other type of cells. However, ohmic loss of electrolyte is dominant performance loss in total SOFC

system which operated low and intermediate temperature. Except high temperature operation, ionic conductivity is bottle neck of the performance for commercialization. So, many researches focused on lowering temperature using extra high ionic conductivity electrolyte materials or ultra-thin electrolyte.

That reason leads to employ anode supported type cell. The anode supported type SOFC cell has some challenges like thermal expansion issues during sintering process (fabrication) and operating process. Thermal expansion problem makes cell durability and stability poor. In this manner, many researchers struggle manage this problems using similar TEC materials between anode substrate electrode and electrolyte or adding another materials for attachment physically powerful. If we control these problems, anode supported type cell takes many benefits. It has thin electrolyte layer that has enough low ohmic loss for high power generation. Also, electrolyte material is most expensive material in cell components. It means anode supported type cell has cost effectiveness.

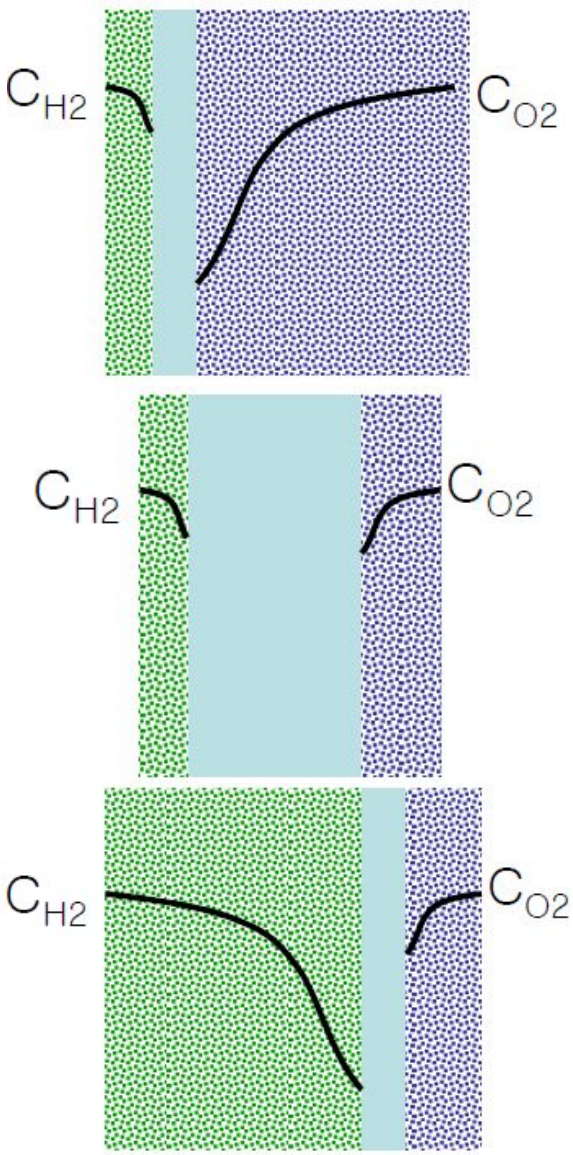

Figure 1.7 Types of mechanical supported cell. (a) the cathode supported type (b) the electrolyte supported type (c) the anode supported type

Chapter 2. Cell fabrication and experimental process

2.1 Cell fabrication and test for verification of YSZ-GDC bi-layer

We selected high conductive electrolyte material and functional layer structure for lowering operating temperature and preventing chemical stability. A core electrolyte material was GDC that have low ohmic resistance in low operation temperature rather than YSZ material. Between anode side and GDC electrolyte, YSZ functional thin layer was deposited via ALD technique.

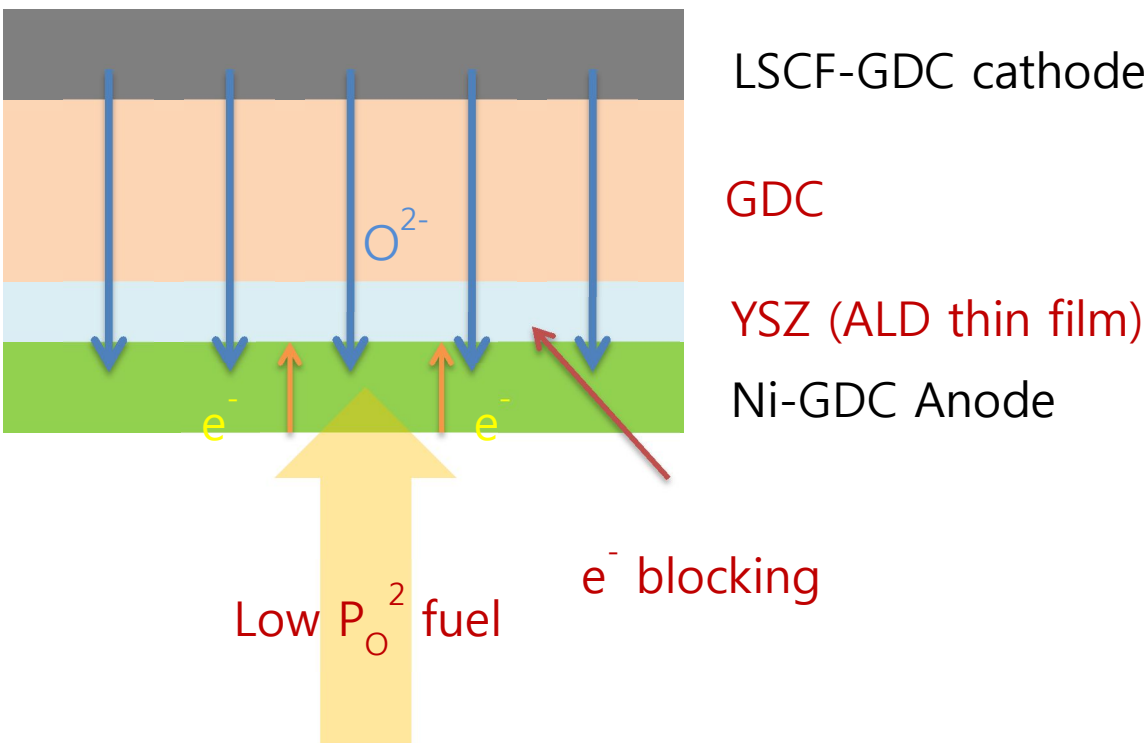

Figure 2.1 Schematic of a YSZ/GDC bi-layered electrolyte SOFC

2.1.1 The components of bi-layered electrolyte

ALD deposition technique is high-cost and slow process, but it can control layer thickness and material composition straightforwardly. So, we use this process for verification of effect of YSZ-GDC bi-layer cell.

We chose electrolyte supported type SOFC cell in this verification. The electrolyte supported type SOFC and make easily. The electrolyte substrate is made by sintering core electrolyte material. On the electrolyte substrate, functional layer, anode material and cathode material are deposited, respectively.

2.1.2 ALD-YSZ for a functional layer

A key point of this study is the YSZ ALD deposition layer on anode side of GDC electrolyte. The ALD-YSZ layer is necessary thickness minimizing for effective performance. The minimized YSZ thickness means we can obtain fast ion transport with minimized ohmic loss in lowered operating temperature. ALD device have ability of Sub-nm thickness control for thin layer. Also the ALD can guarantee precise thickness control which means repeatability and uniform quality. Moreover, ALD's high density and good step coverage promise blocking the direct contact of hydrogen so that it protects ceria from reduction environment. In addition, we thought that chemical and mechanical stability of YSZ could help that increase durability of the whole cell. Last of all, we expected YSZ's high electron insulation property could block the electron over flux through GDC electrolyte in low p_{O2} atmosphere and protect from the reduction of ceria. And we conducted a case study to confirm maintaining the functionality of ALD-YSZ like bulk YSZ. Prinz et al. in Stanford University composed 60nm ALD-YSZ electrolyte with Pt electrodes. They succeeded to operate this μSOFC at below 500°C. [56] So we can confirm that there is no problem using ALD-YSZ for functional layer.

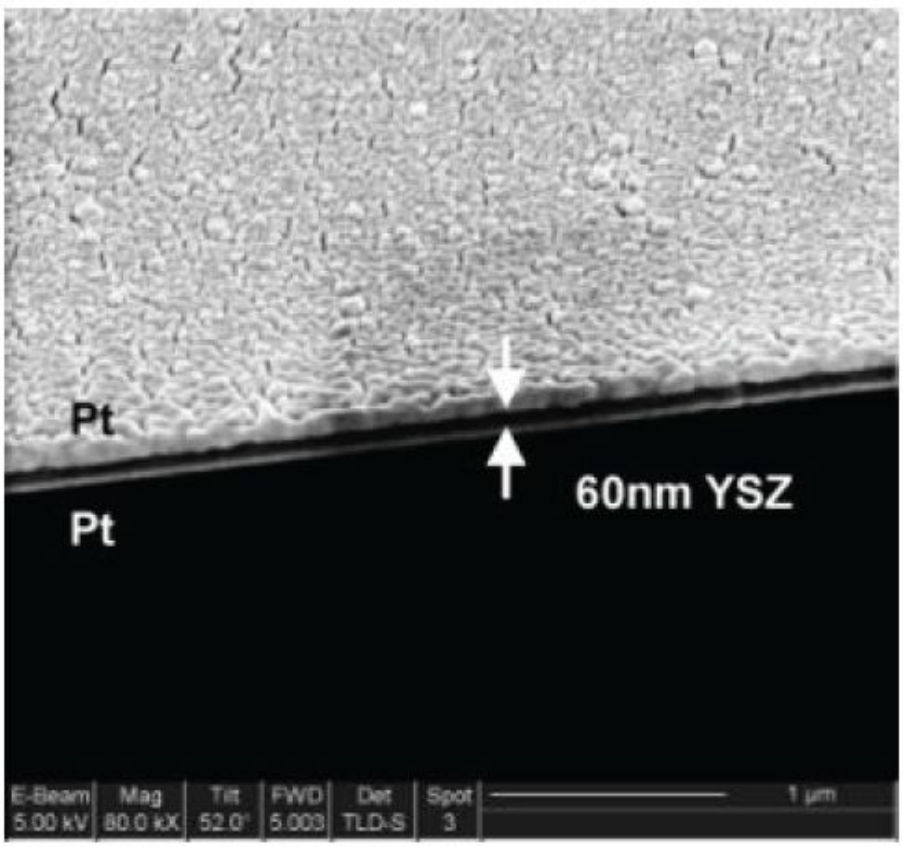

Figure 2.2 Example of ALD-YSZ based μSOFC [56]

2.1.3 Cell fabrication

To carry out the investigation focused on the electrolyte, we planned experiments with electrolyte-supported button cells although the performance would be much poorer (about 500μm thickness electrolyte) than that of typical anode-supported cells.

For SOFCs thin electrolyte directly connects to high performance because ohmic loss is the major polarization factor of SOFCs. So the thinner electrolyte you choose, the lower performance loss can be appeared. Typical electrolyte thickness is under 50μm.

For preparing electrolyte substrate, densified 10% gadolinia doped ceria $(Ce_{0.9}Gd_{0.1})O_{1.95}$ in the form of disks with 1 inch diameter and 3mm thickness were obtained from NexTech Materials, Ltd. Then the disks were ground to 200 and 500μm thickness and polished with diamond sand. (200μm type cannot be used in experimental because of the breakage during the pressing process for sealing) After a thermal etching process of GDC disks at 800°C for two hours that can eliminate the grinding oil or sticky components, the roughness was measured to be 134nm RMS value.

The coating of YSZ on GDC disks was conducted via ALD process with a zirconium precursor (Tetrakis (dimethylamido) zirconium, $[(CH_3)_2N]_4Zr$, Sigma-Aldrich® and with a yttrium precursor (Tris (methylcyclopentadienyl) yttrium, $(CH_3C_5H_4)_3Y$, Strem Chemicals Inc.).

Deposition conditions were below. The temperature of the ALD reaction chamber was 230°C, and distilled (DI) water was used as an oxidant. [58] For 8 mole %, cycle ratio was 7:1. The YSZ deposition rate was 1.4~1.5 Å per cycle.

After deposition, the annealing process follows at 800°C. The final electrolyte samples were 500μm pure GDC disks without coating, 345 cycles (50nm) ALD-YSZ film coated 500μm GDC disks, 690 cycles (100nm) ALDYSZ film coated 500μm GDC disks and 1380 cycles (200nm) ALD-YSZ film coated 500μm GDC disks.

Then, the electrode materials of GDC-NiO cermet for anodes (50:50) and GDC-LSCF for cathodes (50:50) were applied to all the electrolyte samples. The anode was screen-printed on the electrolyte and sintered at 1400°C for 2 hours. The cathode was applied according to the similar procedure but sintered at 1200°C for 2 hours. The heating and cooling rate was 3°C/min and it was enough to release internal residual stress. So we could confirm that there was no crack or fracture in the fabrication process and in the final cells. The dimension of electrodes was 1cm by 1cm and each thickness was about 30μm. To protect the ceria electrolyte from reducing environment, the anode was attached to the YSZ coated side. (Figure. 2.3)

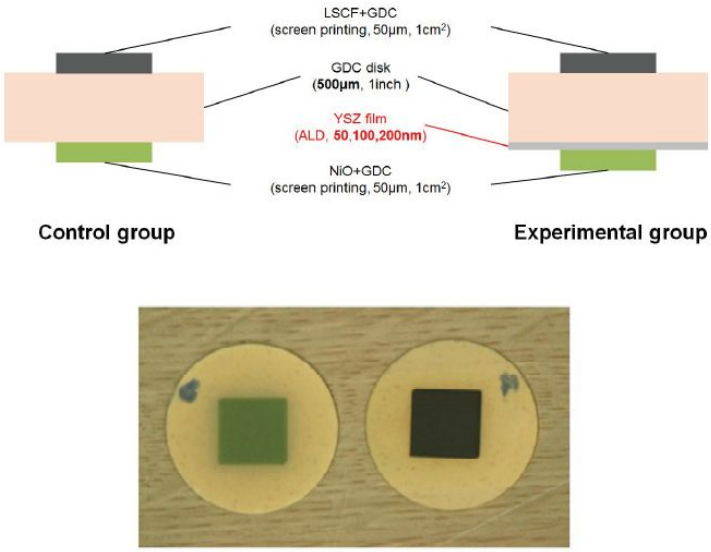

Figure 2.3 Schematics of the ALD-YSZ / GDC cell and the pure GDC cell and actual image of the anode and cathode sides

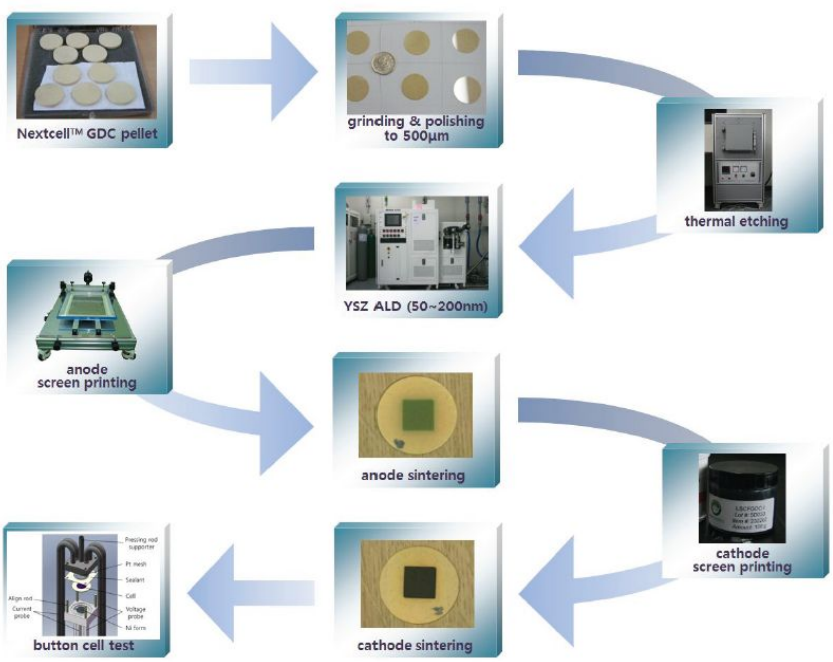

Figure 2.4 ALD-YSZ bi-layered cell fabrication procedure

2.1.4 Cell test procedure

The button cell test station was composed of an electric furnace (Korea Furnace Development Co., Ltd.) with temperature controller (Yokogawa, UP550-01), Thermo couples with indicator, cell pressing unit, gas tubes with mass flow controllers (MFC: Mykrolis, FC-280SAV), humidifier in the anode line, electrochemical measurement devices (Solartron, SI 1287 and SI 1260), and cell supporting fixture. (Figure 2.7)

Electric furnace should have minimum internal volume that can accommodate supporting fixture only. If furnace is big, internal might not follow controller's target temperature. Thus it can delay experimental time and affect cell degradation. Furnace controller should be programed to have several temperature segments for sealant de-binding process. Thermo couples (TC) used to measure the temperature of fixture. Because the Furnace temperature could be different from actual cell temperature, K type thermocouple is used in contact with the fixture. Cell pressing unit is the device to give weight to cell to ensure gas sealing. Rotating handle controls pressure for whole cell sealing. The load cell at the end of pressing unit senses is employed. We used 3 kinds of MFC for hydrogen, nitrogen and air. They can control the flow from 0 to 500sccm. Air tube to cathode side also should be connected to anode side because gas should be flow in the fixture at the anode and cathode side in de-binding process. Nitrogen and hydrogen line to the anode side should be merged so that we can control the hydrogen concentration in operation. The bubbler in anode line humidified (about 2% AH) the fuel gas. The gas regulator maintains the pressure of feeding gas. We could measure cell voltage, current and impedance data with electrochemical measurement devices. They connected to the cell supporting fixture by 4 probe type or 2 probe type.

The cell supporting fixture design shown in Figure 2.8 was made of Inconel 600 for long time stability. It was fitted to sheet type sealant which was easily removable after the operation. And it needed to press for gas sealing. This fixture consisted of upper and lower structures that were assigned to cathode and anode. The structures include current probes that are rod-shaped to minimize the iR drop and voltage probes that are pipe-shaped to provide fuel and oxidant. Ni form on the anode side and Pt mesh on the cathode side are placed as flexible current collectors according to pressing situation.

This design and small furnace can guarantee fast response to furnace temperature control and need special additional structure on top of furnace. Figure 2.8 shows the cell performance comparison between commercial data and experimental results on this fixture. We got the good results at 650°C and 700°C so that we could trust this fixture system. The performance gap at 800°C came from that the sealant capacity was limited to 700°C.

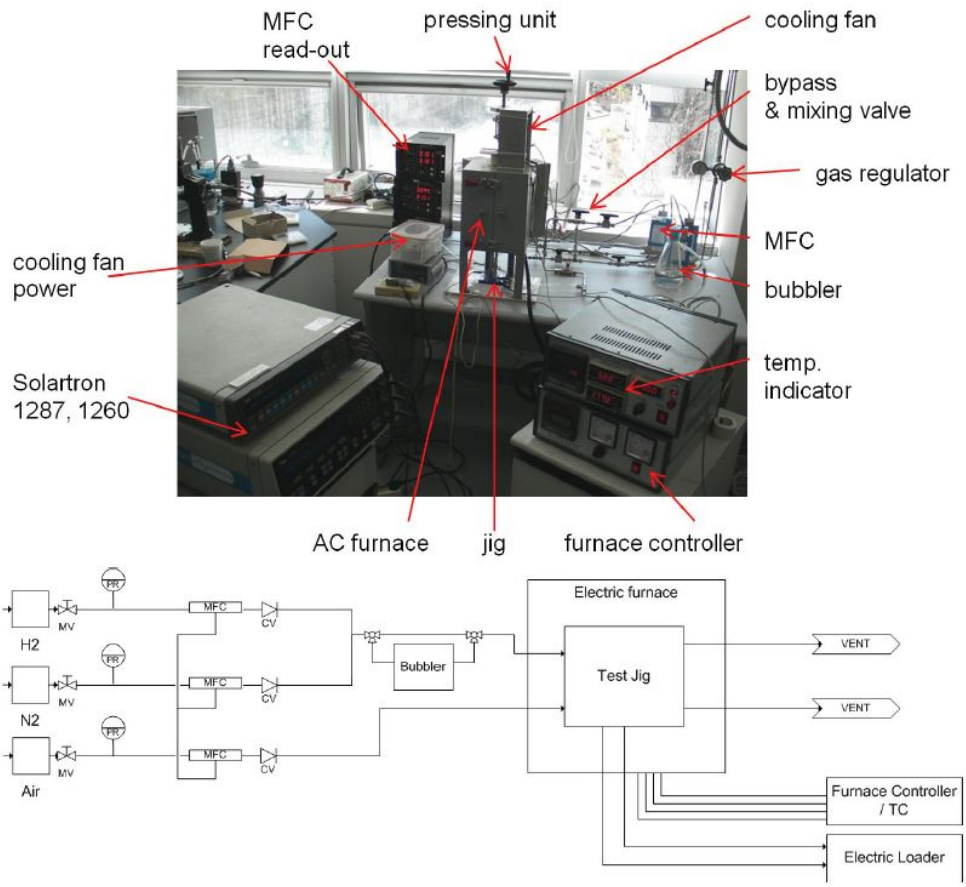

Figure 2.5 Button cell test station and P&ID diagram

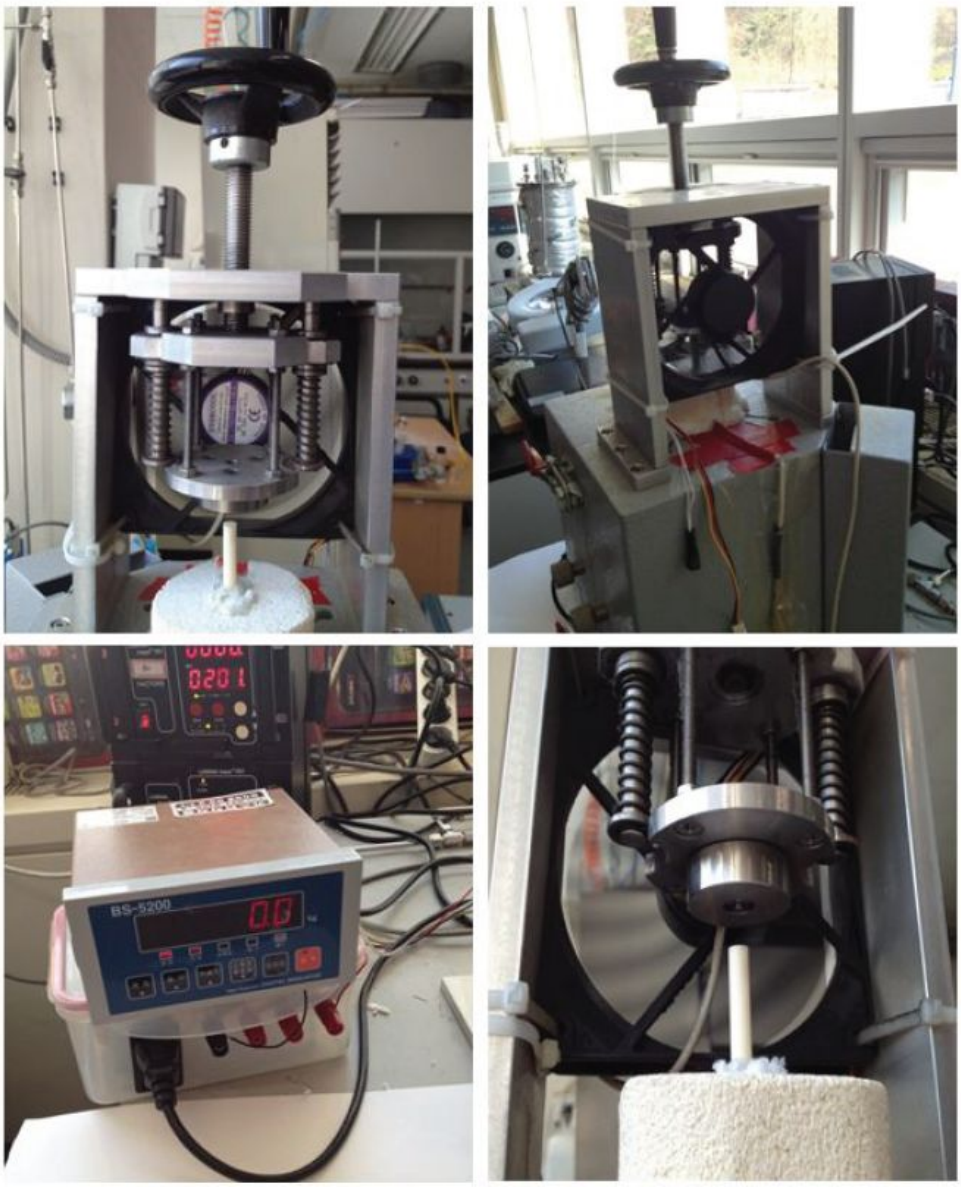

Figure 2.6 Cell pressing unit and indicator

Figure 2.7 MFCs and controllers

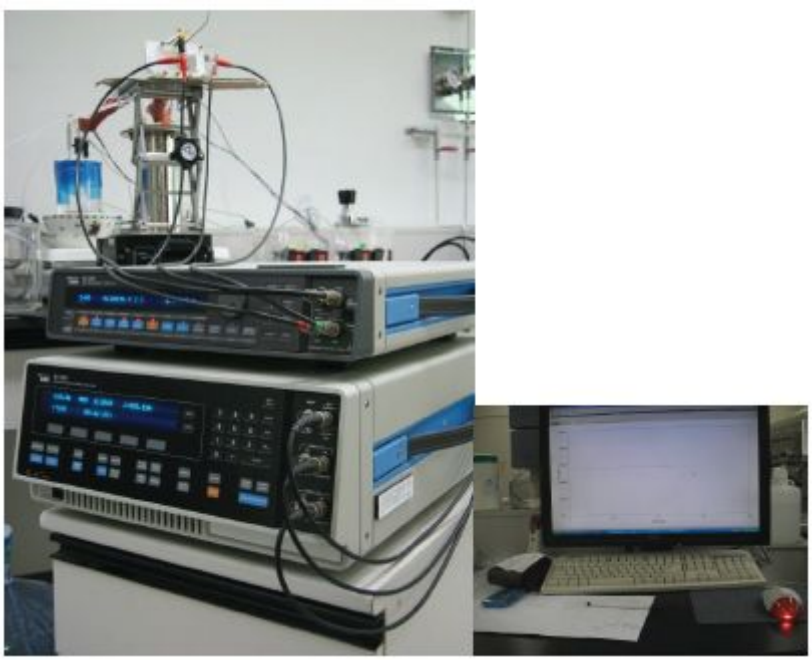

Figure 2.8 Solartron SI 1287 and SI 1260

Before heat up, preparation process on this fixture followed this order. First we cut a Ni form into the shape of groove of bottom fixture and pressed it to the thickness of groove. And we put the button cell on the Ni form. After putting alumina align rod into the hole, sheet type sealant was placed. Sealant sheets were laminated 2~4 times. Lamination process was done on 80°C at the hydraulic press. We pressed Pt mesh to the thickness of 80% of sealant because thickness of sealant reduced in de-binding process. The reason of same thicknesses of sealant and Pt current collector is to get the gas tightness and to secure contact between cathode-Pt mesh – upper fixture. If Pt mesh was thicker than another, gas sealing could not be accomplished. Otherwise, thicker sealant cause open circuit situation so that we cannot measure the cell performance. Putting the upper fixture according to the align rods is the final stage of fixture preparation. Figure 2.9 shows the experiment preparation process on this fixture.

The furnace was controlled to heat up slowly to prevent thermal stress and breakage of GDC and to de-bind the organic components in sealant. (Figure 2.14) The heating time was over 18 hours to reach the operating temperature of 600°C. For the sealing property, we maintained temperature for several hours at 170°C, 250°C, 350°C, 500°C, and 620°C during hear-up schedule. Cells were compressed lightly between upper and lower supporting structures to ensure gas tightness at the cell sealing. We started increasing pressing load from 0.1kgf/cm2 at 530°C to 1kgf/cm2 at softening temperature (580°C).

Till the operation temperature, air feeding to anode and cathode side should be done to remove the organic components generated from de-binding process. To prevent sudden oxygen partial pressure changes and to promote reactions on anodes, we humidified the gas fed to the anode with bubbler (2% AH) from the

anode-reduction step until the end of the experiments. Also, we carried out a slow anode-reduction process for 8 hours with low hydrogen concentration gas (5% H_2 and 95% N2). Current-voltage (iV) characterization and electrochemical impedance spectroscopy (EIS) with 100% H_2 fuel gas followed the anode-reduction.

Then we cooled down the furnace slowly feeding H_2 to preserve the changes of electrolytes from reducing environment without thermal stress.

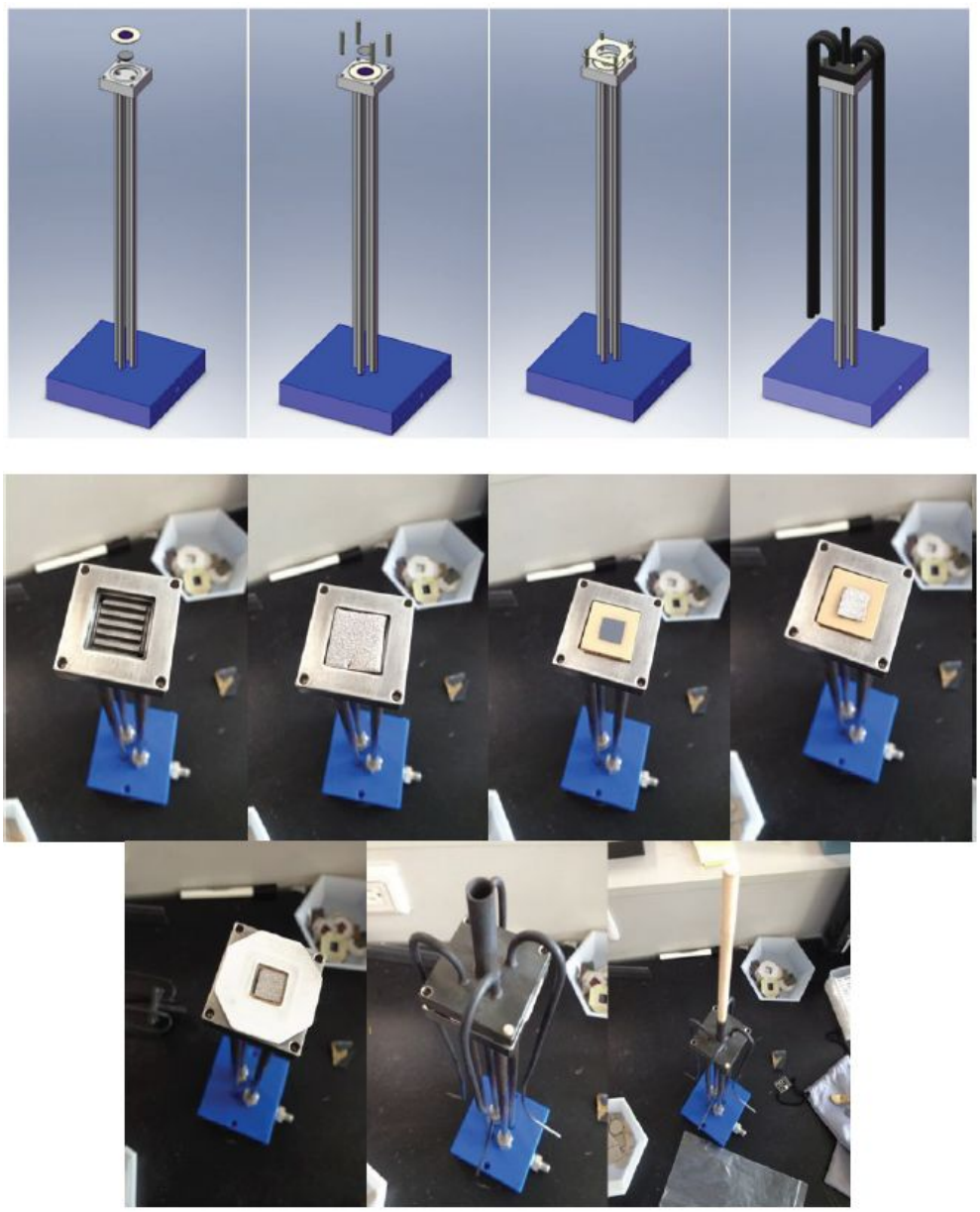

Figure 2.9 Experiment preparation process on the fifth design fixture.

2.1.5 Result of ALD-YSZ/GDC bil-layered cell test

2.1.5.1 Confirmation of the ALD-YSZ layer

We could confirm that the thickness of the as-deposited 1380 cycles ALD-YSZ layer on bulk GDC electrolyte pellet before electrodes sintering step (Figure 2.15(a)) was about 200nm from the cross section scanning electron microscope (SEM) images with focused ion beam (FIB: FEI, Quanta 3D FEG). From this image, the ALD-YSZ recipe on GDC was successful so we could find out that the growth rate, layer shape, thickness uniformity, and good step coverage were as expected. Together with the FIB-SEM image that includes more backscattered electron (BSE) signal which enabled to distinct YSZ from GDC via high contrast, we could obtain more magnified SEM image (FEI, Strata 235DB dual-beam FIB/SEM) with through the lens detector (TLD) to see the morphology of as-deposited ALD-YSZ film which has pillar-shaped nano structure. (Figure 2.15 (a′)) Then we obtain the FIBSEM image of the 690 cycles ALD-YSZ layer after the operation. After the operation means YSZ film on GDC suffered electrodes sintering processes (1400°C and 1200°C) and 3 days operation with hydrogen gas. Shown in Figure 2.15 (b) dark YSZ was deposited on GDC as a layer shape with perfect step coverage, too. But the thickness was about 85nm which was less than 100nm of as-deposited step. We thought the reason of this gap came from the slight mixing of YSZ and GDC on electrode sintering temperature. We will discuss this phenomenon later.

Then we performed X-ray photoelectron spectroscopy (XPS: Kratos Analytical, AXIS-HSi) analysis of the surface of bi-layered electrolytes. ALD-YSZ as-deposited and after the cell operation samples were investigated, too. Figure 3.16 shows clear peaks of yttrium and zirconium for the surfaces of the sample

before electrodes sintering and after the operation. The red letters show the locations of main peaks for Ce, Gd, Zr, and Y elements. [59] There is no peak at the location of Ce and Gd., so there was no peak related to gadolinium and cerium. So we could know YSZ covered GDC surface and there was no change after the exposure to high temperature and to reducing gas. Figure 3.12 shows depth profile of bi-layered electrolyte which was deposited 345 cycles (50nm) ALD-YSZ. (PHI, VersaProbe Scanning XPS Microprobe) We could confirmed about 8% (7~8.2%) yttrium mole fraction in YSZ thin layer until 2 min etching. And we could make sure the 50nm Thickness of ALD-YSZ layer from the experiences of YSZ etching rate about 25nm/·min with the condition of 5kV beam energy, 1μA beam current, and 1μm X 1μm spot size.

From these SEM and XPS results, we conclude that nano-scaled ALDYSZ layer could survive the electrode sintering condition of 1200°C and 1400°C as well as the cell operating condition in the reducing atmosphere maintaining its shape and conformability with identical composition ratio as we expected.

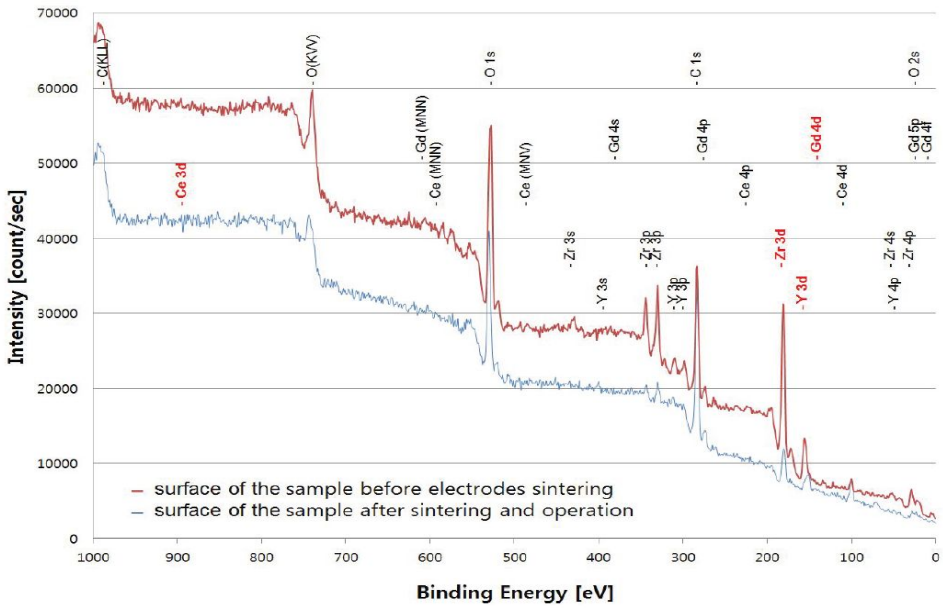

Figure 2.10 XPS spectra on the surfaces of ALD-YSZ / GDC samples (red) before the electrode sintering process and (blue) after the cell operation

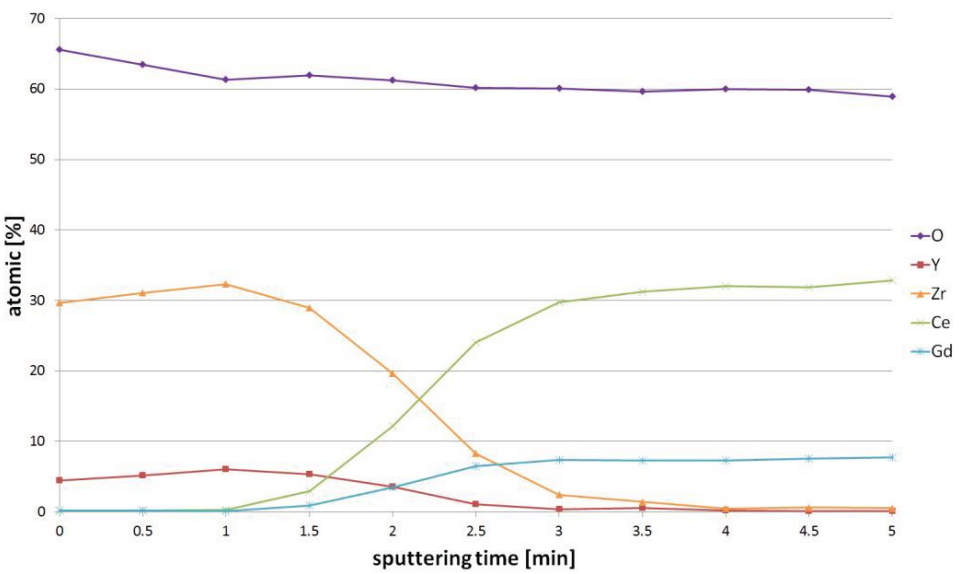

Figure 2.11 XPS depth profile of the bi-layered electrolyte which was 345 cycles (50nm) ALD-YSZ coated GDC

2.1.5.2 OCV transition result

We investigated the open circuit voltage (OCV) changes of the fabricated cells at a low hydrogen concentration (5% H_2, 95% N2) corresponding to the anode-reduction step prior to cell operations. As shown in Figure 2.18, at 620°C the pure GDC electrolyte cell showed a voltage drop and saturation at 0.8V after 8 hours from hydrogen feeding whereas the 690 cycles (100nm) YSZ-coated GDC cell showed constant 0.95V. This difference was due to the increase of electronic conductance on the hydrogen side in the electrolyte from the gradual expansion of the domain of reduced cerium ion for pure GDC cell. The voltage of 0.95V could not reach the reported calculation value over 1.0V for humidified hydrogen fuel gas, [60],[61] but we could corroborate the long term electron insulation effect of nano-scale YSZ layer considering typical experimental data for ceria based cell's OCV varied from 0.87V to 0.91V. [62],[50] We could know that the electronic conduction was not perfectly blocked, because typical OCV values from YSZ cells exceeded 1.1V on this temperature even though their results were from the stack scale experiments. [63] Also, at higher hydrogen concentration, during the anode-reduction steps of the 100nm YSZ-coated cell, the OCV drop was observed. So we thought more experiments considering electrolyte thickness variation via ALD were needed for the optimization.

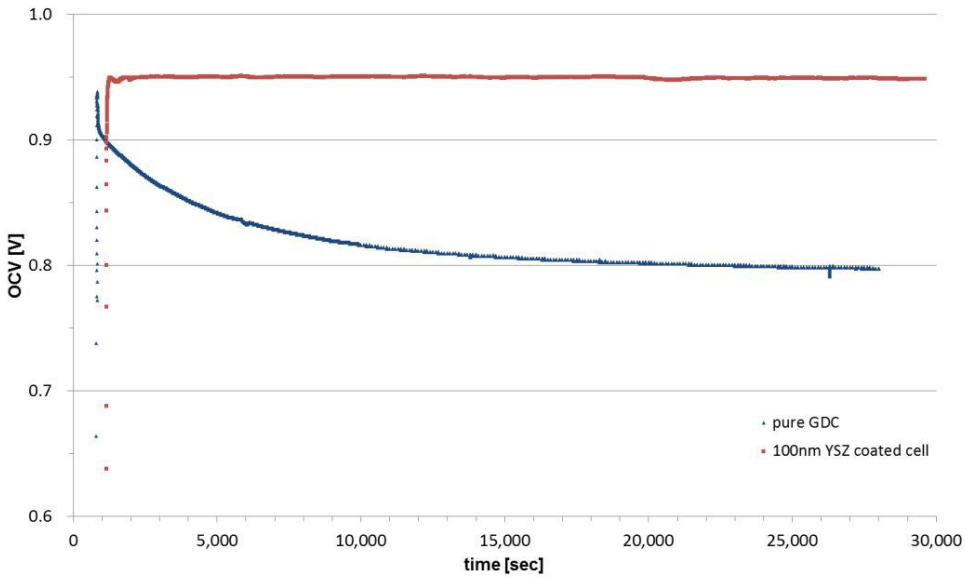

Figure 2.12 OCV transitions of the pure GDC cell and of the 690 cycles (100nm) ALD-YSZ / GDC cell at 620°C using 5% H_2 fuel during the anode reduction step

2.1.5.3. iV and power density results

After the observation of OCV transition for about 8 hours, the next experiment was iV and power density measurement at 600°C with the same feed rate of hydrogen and air (200sccm each). The peak power density of the 690 cycles (100nm) YSZ-coated cell was 46.1mW and this cell showed 0.83V OCV. In spite of the low performance, 690 cycles (100nm) YSZ-coated cell showed about 5% higher OCV and 53% larger peak power density than pure GDC electrolyte cell. (Figure 2.19)

Together with above OCV change in Figure 2.18, these results prove the electron insulation functionality of the ultra-thin YSZ layer arising from the ALD method. In the case of the 345 cycles (50nm) YSZ-coated cell, we observed almost similar or slightly lower power density performance compared to the case of the pure GDC cell. The slope of the current density curve was similar to that of the pure GDC cell and the OCV value was slightly higher. This suggests that the electron blocking was meaningless through the 345 cycles (50nm) ALD-YSZ layer, of which the reason was not clear at this point, but further investigation is being conducted.

Figure 2.20 displays a comparison of the iV and power density when the hydrogen and air feed rates were increased to 300sccm. The experiments for the 50nm YSZ-coated GDC cell was excluded since the performance improvement was not observed as explained previously. We observed an improvement in OCV and the power density for the 100nm YSZ-coated cell for increased flow rates, but at the advantageous feed condition for gas, the pure GDC cell did not show any enhancement. We observed the similar trend for other flow rate values, too. Changing the feed rate of gases, we obtained the maximum power of 55.1mW at

0.482V for the YSZ-coated GDC cell under 200sccm hydrogen and 1000sccm air flow rates.

We investigated the performance at various temperatures from 600°C to 700°C and various flow rates. We can confirm that the most effective temperature for YSZ coating was 620°C with 66.7% gap, and that 200/1000sccm (H_2/air) flow rates enhanced the power densities by 19.6%, 35.2% and 414.4% at 600°C, 650°C and 700°C. At 700°C, unstable performance result was due to the temperature limit of sealant and water generation and condensation at the anode side and outlet.

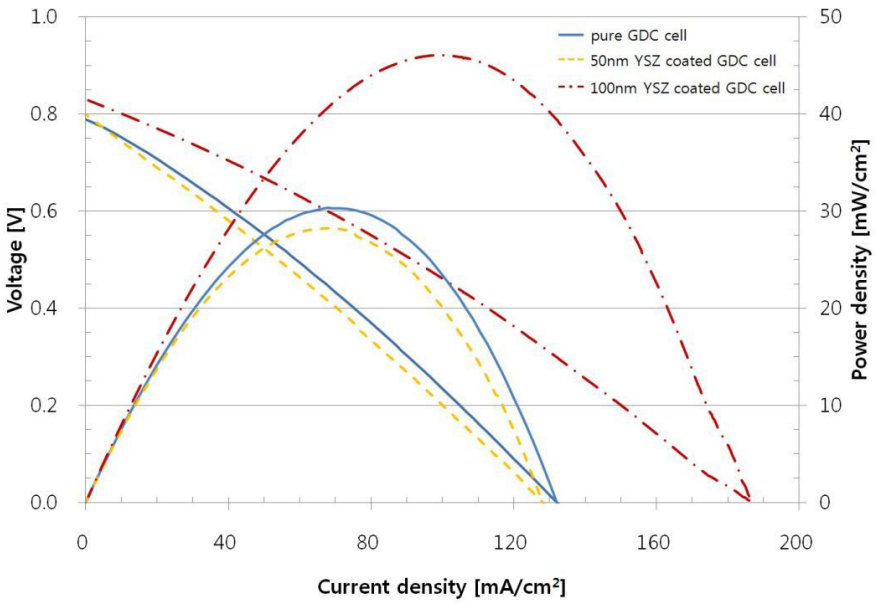

Figure 2.13 iV and power density curves at 600°C for the pure GDC cell, 50nm ALD-YSZ / GDC cell, and the 100nm ALD-YSZ / GDC cell

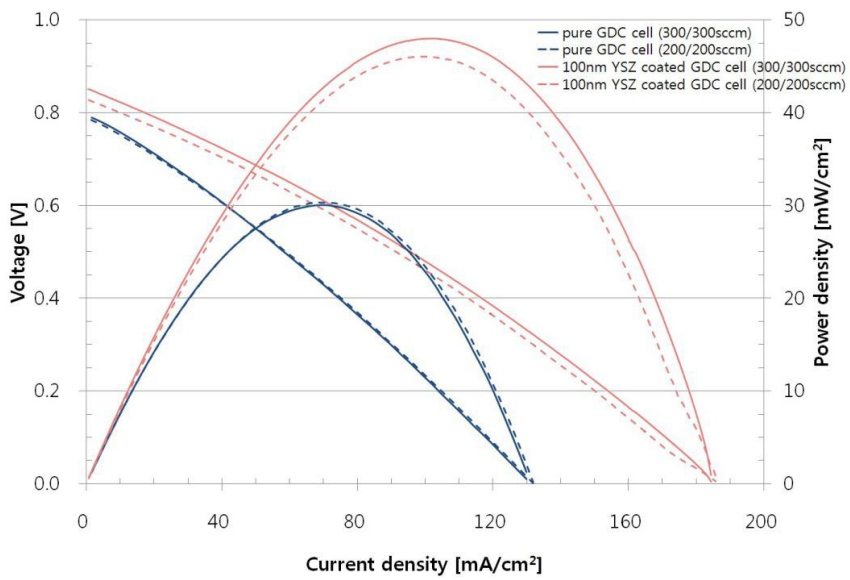

Figure 2.14 Comparison of the iV and power density at 600°C as the hydrogen and air feed rates increased from 200sccm to 300sccm

2.1.5.4 EIS spectra results

We investigated the effect of the ALD-YSZ functional layer from measuring the electrochemical impedance of the same samples. The gentler slope of the I-V curve for the YSZ-coated cell indicates that its ohmic resistance was lower than pure GDC's. And this observation was confirmed from the EIS Nyquist spectra that were obtained in the frequency range of 2 ~ 106 Hz using the ac amplitude of 30 mV at OCV. In Figure 2.22 (a) the intercept value on real axis of the impedance spectra which means ohmic resistance of cells for the 690 cycles (100nm) ALD-YSZ coated cell was significantly lower than that of the uncoated cell. This was a very interesting result, but the result supports the opposite effect. In general situation, doped ceria exposed to low oxygen partial pressure has both ionic and electronic conductivity. So impedance data must show low ohmic resistance. In addition, because we made cells from pellets of identical thickness GDC, the coated cell which has low conductive YSZ layer must have slightly higher resistance. We thought the reason was that micro cracks were generated at ceria electrolyte near anode due to the long exposure to hydrogen gas so the contact resistance became higher. The enlarged left side half circle in Figure 2.22 (b) than the one in Figure 2.22 (a) that means activation loss of anodes, enabled us to have the same presumption.

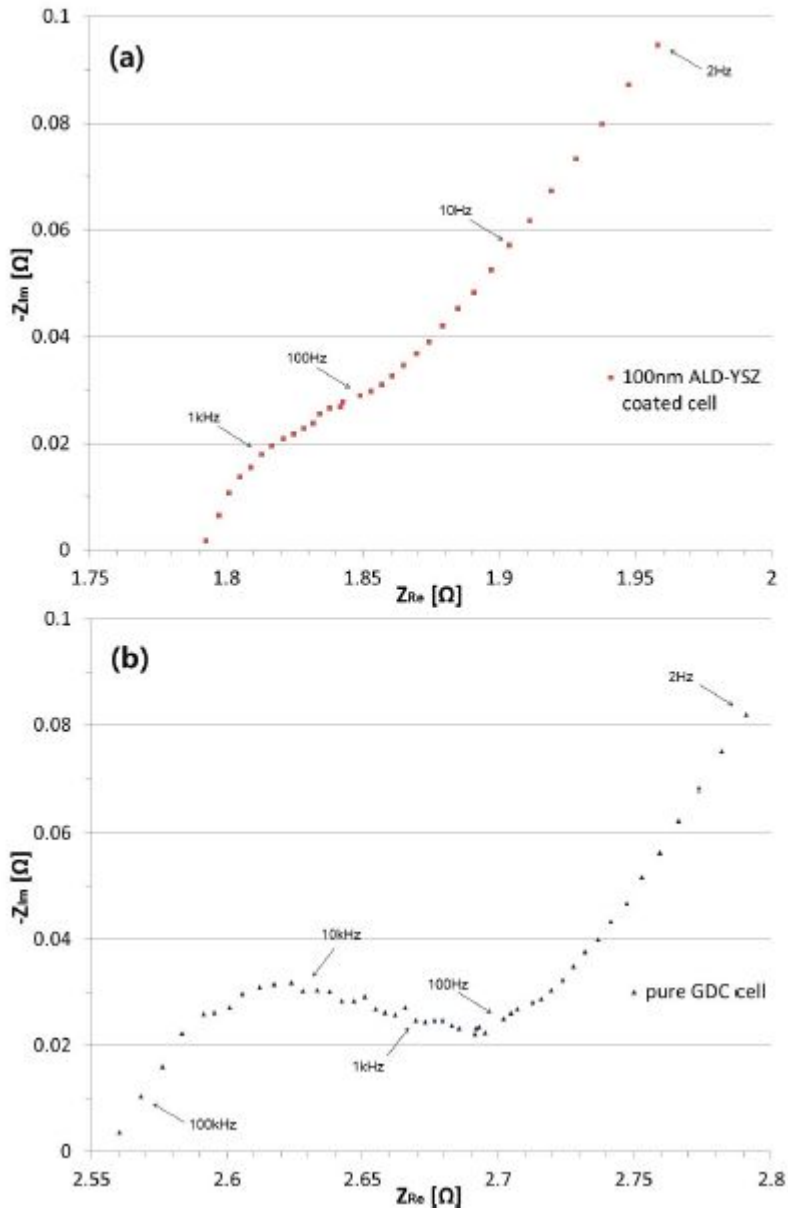

Figure 2.15 EIS Nyquist spectra at 600°C (a) for the 690 cycles (100nm) ALD-YSZ / GDC cell and (b) for the pure GDC cell

2.2 Approach of various anode-supported type SOFC cell fabrication process

As mentioned previously, our goal is to create a solid oxide fuel cell that can be operated on low and intermediate temperature on the possible commercialization. We determined the direction of bi-layer electrolyte for solid oxide fuel cells. We approached another goal of efficient production processes for commercialization. In order to maintain a high power density in intermediate operation temperature, it is advantageous to produce anode supported type SOFCs. To do this, various types of processes for anode supported type SOFC is tried.

2.2.1 Literature survey

2.2.1.1 Wet ceramic process

Wet ceramic process is one of the important and fundamental processes for fabricating SOFCs. However, there are few studies on wet ceramic process for fabrication of YSZ/GDC bi-layer electrolyte cell. Most wet ceramic process studies are focused on GDC material deposition to cathode side to prevent to inter-reaction between cathode material and core electrolyte material. According to the study, such as Ql Liu [56] using spray-coating method one of the wet ceramic process, deposited YSZ and GDC slurry onto prepared anode substrate. A single cell, consisting of a YSZ(～3 μm)/GDC(～7 μm) bilayer electrolyte, a $La_{0.8}Sr_{0.2}Co_{0.2}Fe_{0.8}O_3$–GDC composite cathode and a Ni–YSZ cermet anode is tested in humidified hydrogen and air. The cell exhibited an open-circuit voltage (OCV) of 1.05 V at 800 °C, compared with 0.59 V for a single cell with a 10-μm GDC film but without an YSZ film. This indicates that the electronic conduction through the GDC electrolyte is successfully blocked by the deposited YSZ film. In spite of the desirable OCVs, the present YSZ/GDC bilayer electrolyte cell achieved a relatively low peak power density of 678 mW cm^{-2} at 800 °C. This is attributed to severe mass transport limitations in the thick and low-porosity anode substrate at high current densities.

This process, rather than the thin film deposition process proceeds in a simple way, but, rather than cold press process, a lot of the sintering process. The subsequent cost increases, production time is lengthened.

2.2.1.2 Thin film deposition process

Thin film processes have been studied very diverse. Techniques such as chemical vapor deposition (CVD) [16], pulsed laser deposition (PLD) [17], RF magnetron sputtering [18], and atomic layer deposition [ref] have been developed to deposit a thin film of electrolyte.

The thin film deposition process can be extremely precise control. In addition, chamber grows enough, it is possible that produce large scale cell. Moreover, cause this process is a nano-process, it can be synthesis of materials at low temperatures.

However, these thin film deposition method, there are drawbacks. Most of the thin film process is done in a vacuum, so the equipment is expensive and the process time is lengthened. In addition, bulk one cell will be the longer the processing time, because of it is nanometer process.

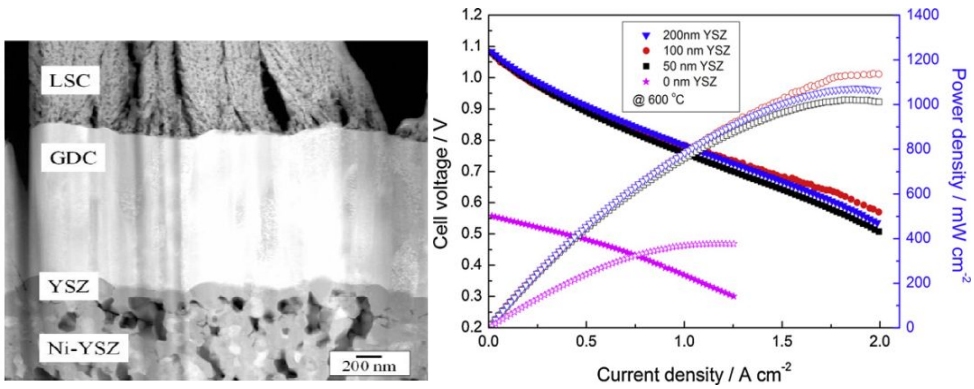

Figure.2.16 ALD bi-layered SOFC SEM cross sectional, power and IV performance[39]

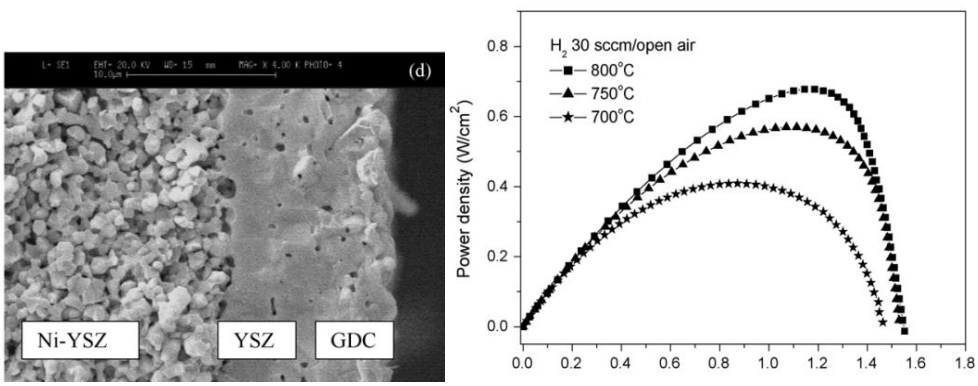

Figure. 2.17 Wet cermic process bi-layered SOFC SEM cross sectional, power and IV performance[47]

2.2.3 Cold press process

There is little research on the production about cold press process with YSZ / GDC bi-layer cell. The cold press process is one of the most fundamental processes in fabricating ceramic products. Conventional cold press process is compacting anode substrate powder and then depositing electrolyte material onto it and re-compacting the whole powders. The thickness of the electrolyte by conventional methods was several tens to hundreds mirco-meters thickness. Conventional cold press process did not use at fine and precision process cause of its difficulty to control. However, Liu eta [65] obtained meaningful results by spray dry coating. Liu eta had succeeded micron deposition by mixed the ceramic powder with ethanol vehicle, and using atomizing nozzle spray. This technique can make micron scale thin layer, moreover can control thickness and uniformity easily. In this study, GDC powder was deposited onto prepared anode substrate and then it was co-sintered for one step sintering process. However, there are not enough studies about fabricating bi-layer electrolyte cell by these cold press processes. So, in this study, we employed cold press process for fabricating bi-layer electrolyte cell anode supported SOFC cell.

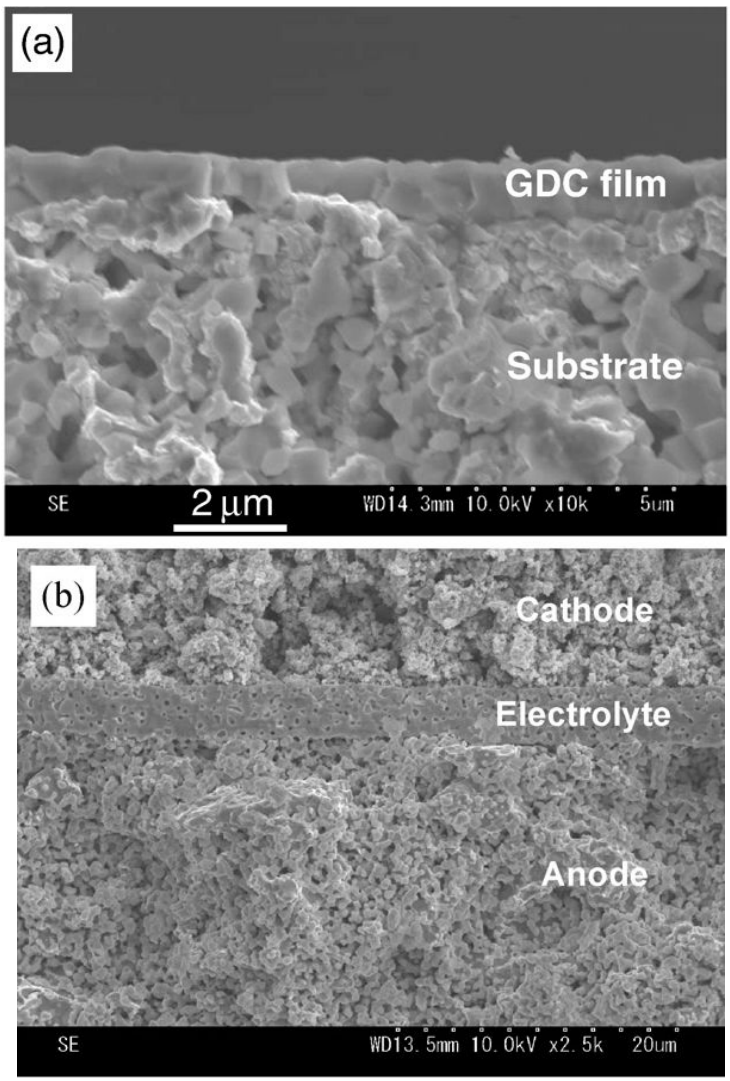

Figure 2.18 Cold press single layer anode supported SOFC SEM cross sectional image[75,76]

2.2.4 Summary of cell fabrication process and Cell test procedure

We studied the production method that can make enough performance at intermediate operation temperature and reduce process cost. As mentioned earlier,, in order to operate intermediate temperature, we prepared cell structure the core electrolyte using GDC material. In addition, in the case of only use pure GDC electrolyte, it is occurred collapse in the lattice structure. And, in the low pO^2 atmosphere, collapse lattice is occured. Moreover, GDC electrolyte material is inter-reaction with LSCF cathode material in high temperature. For this reason, YSZ material is employed as a functional layer. The structure of cell is anode-YSZ-GDC-cathode,

In addition, the thickness of the electrolyte affect to the cell performance closely. When the thickness of the electrolyte is increasing, the ohmic potential is rising, and it affect to reduce cell performance. It is shown at Figure 2.28. This figure is calculation that assumed electrolyte and electrode are identical matieral, and thickness of anode supported cell is assumed 500(Anode) – 50(Electrolyte) – 50(Cathode) um respectively, electrolyte supported cell is assumed 50(Anode) – 500(Electrolyte) – 50(Cathode) um respectively.

The main equation is as following.

The ohmic voltage is following

$$\eta_{ohmic} = jR = j\frac{t^M}{sigma} = j\frac{t^M T}{Ae^{\frac{\Delta G_{act}}{RT}}}$$

The cathodic and anorthic over voltage is following

$$\eta_{cathode} = \frac{RT}{4\alpha F} \ln \left[\frac{j}{j_0 p^C \left(x_{O_2}|_d - t^C \frac{jRT}{4Fp^C D^{eff}_{O_2,N_2}} \right)} \right]$$

The overall over voltage is following

$$\begin{aligned} V &= E_{thermo} - \eta_{ohmic} - \eta_{cathode} \\ &= E_{thermo} - j\frac{t^M T}{Ae^{\frac{\Delta G_{act}}{RT}}} - \frac{RT}{4\alpha F} \ln \left[\frac{j}{j_0 p^C \left(x_{O_2}|_d - t^C \frac{jRT}{4Fp^C D^{eff}_{O_2,N_2}} \right)} \right] \end{aligned}$$

It is simple result that is assumed ignoring mass transfer over voltage in electrode side, but, it can be shown an effect of electrolyte thickness to cell performance roughly.

Based on these results,, in order to get higher power density than one of previous method, we made SOFC cell with anode supported bi-layer electrolyte structure.

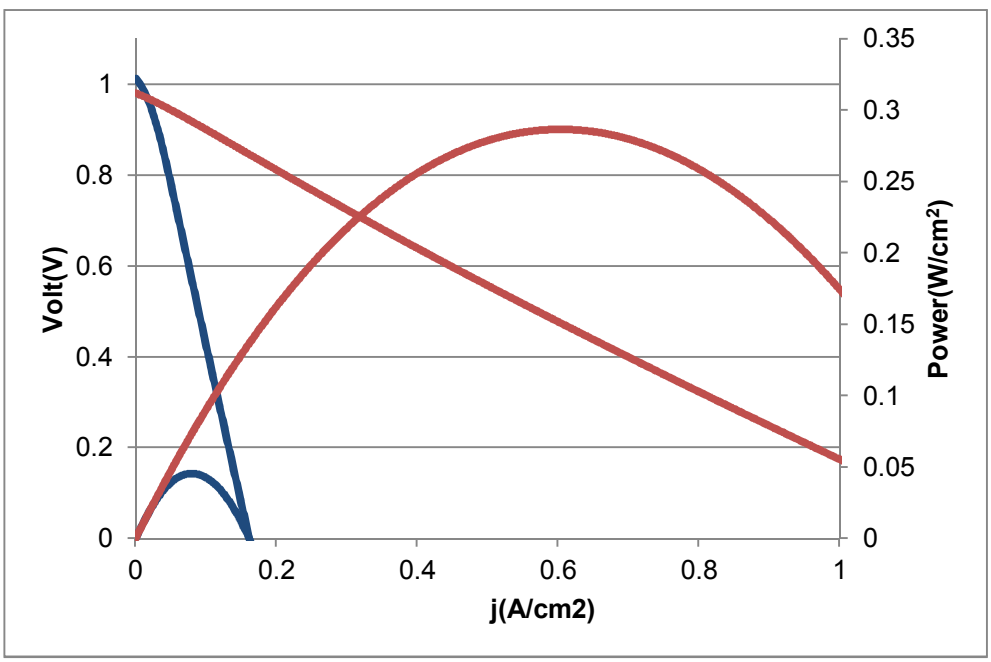

Figure 2.19 Power density and IV curve of Electrolyte supported cell and Anode supported cell.

2.2.4.1 Summary of cell fabrication

We have access to a variety of ways to produce the anode supported bi-layer electrolyte cell. (Table 2.1)

The first way to try is preparing baked anode substrate, and depositing electrolyte material by wet ceramic process. The way to fabricate anode substrate is cold pressing anode substrate material and baked it to make green body. This prepared green body is cut and polished for adequate thickness and roughness. This process has some advantage that can be obtained uniform and thin substrate. We deposited electrolyte onto this prepared green body anode substrate by wet ceramic process.

We used one of the wet ceramic processes, screen printing method, dip coating and spray coating. The electrolyte slurry recipe for wet ceramic process is shown at Table 2.2.

The second way to try is fabricated coin cell substrate one by one using steel die. 24mm diameter steel die is employed. We located anode substrate powder in the steal die, and then densify the powder by cold pressing, and then calcined it. The electrolyte was prepared as same manner,

The advantage of this method is that the whole process is can be reduced by reducing the cutting process. In addition, cutting and polishing processes can make stick additional impurities to the surface. The result of the impurities have to be removed by sintering or calcinning, these materials can be a contamination source in depositing electrolyte materials. And, this contamination leads to reduce cohesion between intersurface of materials. Table 2.1 is how to make the anode supported cell with various.

In the first cutting substrate way, there was not only aforementioned contamination problem, but also residual stress and rough surface problem due to cutting and polishing processes. It leads to very serious warpage problem during cell sintering process.

In the second substrate way, we employed spray dry coating and obtained the highest performance than other way to make unit cell.

We obtained 87mW/cm^2 at 600^{o}C using GDC10 electrolyte material, and 160mW/cm^2 at 600^{o}C using GDC10 electrolyte material. The figure 2.29 is shown the IV and power density results of GDC20 electrolyte material cell. And, the figure 2.30 is shown cross sectional SEM image of it. We can find 40um electrolyte and every layer is well boned and crack free.

Table 2.1 Summary of fabrication approaches

Substrate	cutting and polishing							pressing	
Type	Square	Coin							
Diameter (mm)	20	32		25					
Thickness (mm)	1	0.5	1	0.5	1	2	2		
Electrolyte	Screen printing				Dip coating	Spray coating			
Material	GDC10					GDC10	GDC20	GDC10	GDC20
Power density at 600°C (mW/cm²)						20	15	87	160
	Crack	Warpage							

Table 2.2 The electrolyte slurry recipe for wet ceramic process

	function	slurry(g)	spray(g)	function	slurry(g)	function	spray(g)
GDC10	Ceramic powder	40	2	GDC10	600	GDC10	10
Trichloroethylene	Solvent	24	4	Terpineol	100	Ethanol	100
Propanol	Solvent	6	36				
Cornoil	Dispersant	2	0.1	Polyvinyl pyrrolidon	0.2	Cornoil	0.1
Benzyl butyl phthalate	Plasticizer	2	0.1			Terpineol	2.35
Polyethylene glycol	Plasticizer	2	0.1				
Polyvinyl butyral	Binder	1.4	0.07	Polyvinyl butyral	1.8	Ethyl cellulose	0.15

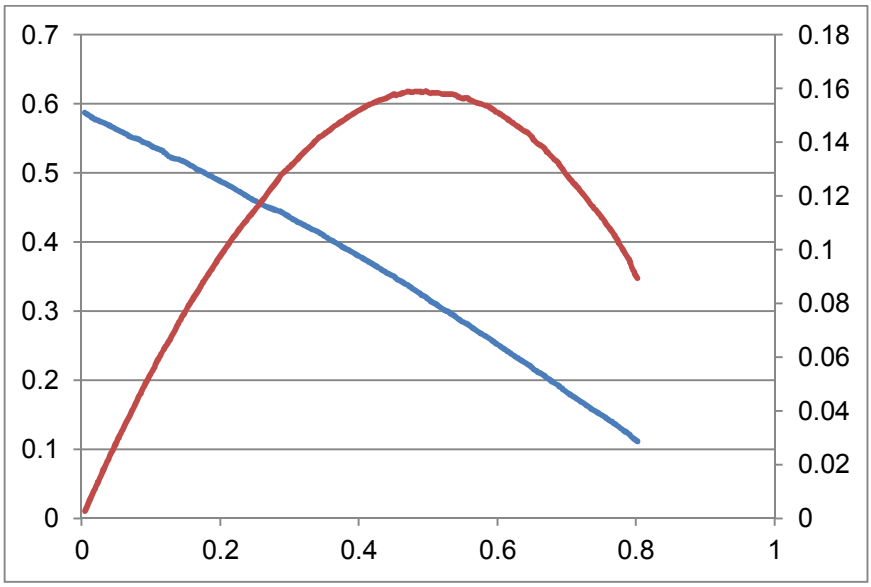

Figure 2.20 IV and power density of spray coated electrolyte cell, 600℃ humidified H_2 : 100 SCCM N_2 : 100 Air : 100 SCCM

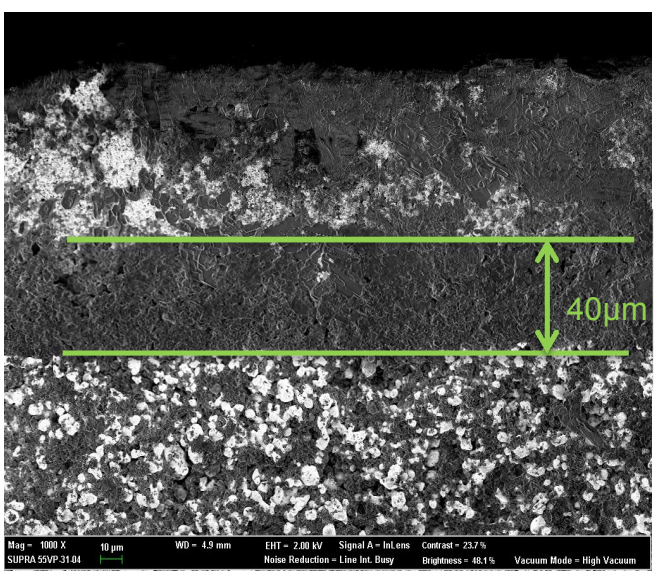

Figure 2.21 Cross sectional SEM image of the spray coated electrolyte

2.2.4.2 Test procedure of anode supported type SOFC unit cell via Cold press process

We modified some components of previous bi-layer verification test setting. Previously test, we employed glass fiber type gasket for gas sealing. However, modified test setting, it is used gold ring as a sealant. The single cell was sealed using a gold ring on one end of an INCONEL fixture. Dimension of the gold ring is 15mm ring diameters and 0.5 mm wire diameters. The surface of outer side of gold ring was coated ceramic sealant (Aremco 503) to prevent leakage of hydrogen. Platinum meshes were used as current collectors. The single cell was pressured by a bolt of jig. After the in situ reduction of the NiO anode in H_2 for several hours, the performances of the cell were measured at various temperatures from 600 to 800°C. Hydrogen passed over the anode at a flow rate of 100 sccm with 3% H_2O, and air flowed over the cathode surface at a flow rate of 100 sccm. The impedances were measured typically in the frequency range from 0.05 Hz to 50 kHz under open-circuit conditions using a Solartron 1287 potentiostat and 1260 frequency-response analyzer. The tested cell was fractured and examined by a scanning electron microscopy (SEM). The SEM observation was performed on a scanning electron microscope (SUPRA 55VP, Carl Zeiss).

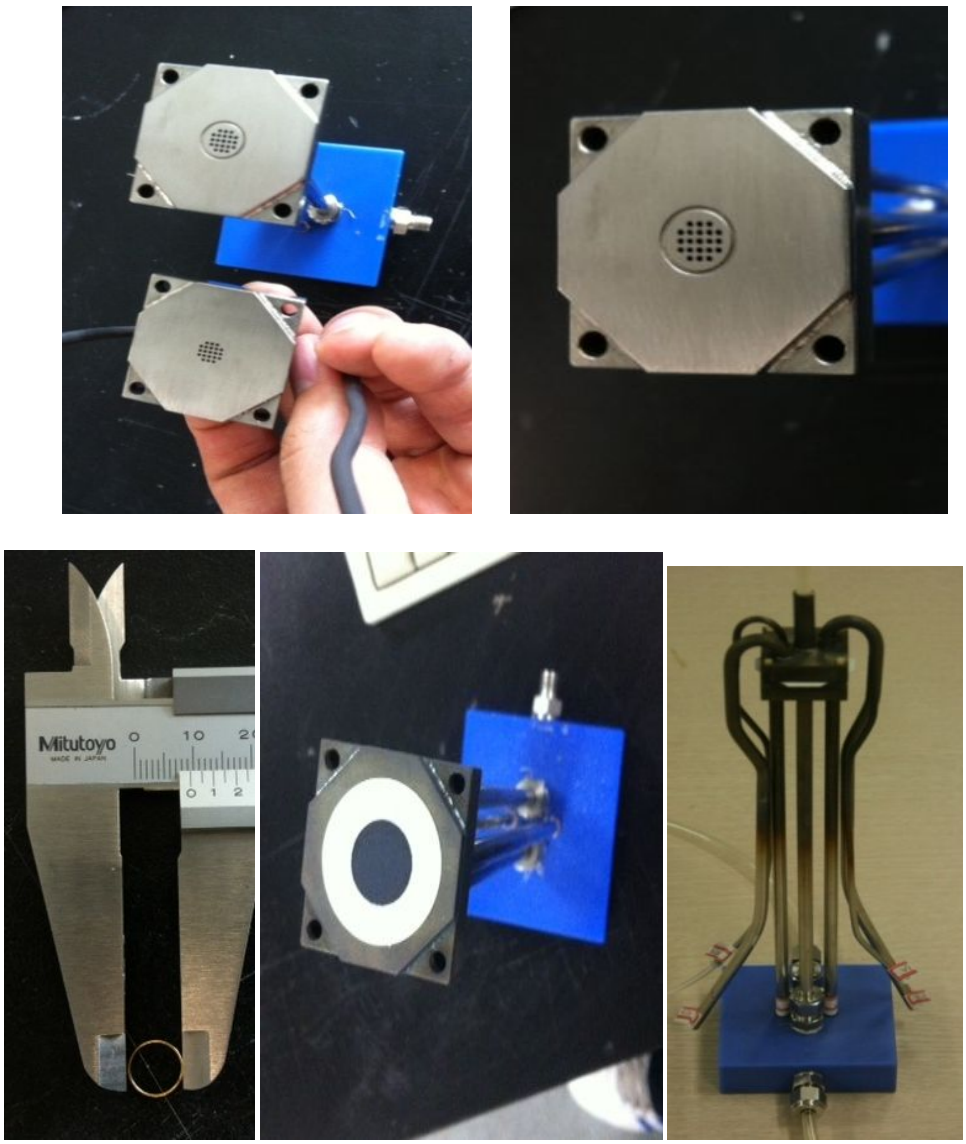

Figure 2.22 Modified test fixture using gold ring sealant

Chapter 3. Test of the YSZ/GDC bi-layered electrolyte anode supported type cell via cold press process

3.1 Introduction

Solid oxide fuel cells (SOFCs) are one of more promising technology for mobile and stationary applications. Decreasing the operating temperature of SOFCs from conventional to an intermediate temperature can offer many advantages. Low material temperature degradation, high system reliability, and long stack life time can decrease interconnect materials and fabrication costs. Significant efforts have been achieved to lower the operating temperature of SOFCs [1-6]. Three methods have been adopted to reduce the electrolyte thickness that uses new electrolyte materials with high ionic conductivity at a lower temperature, and declining polarization resistance in an intermediate temperature. Doped ceria (CeO2), which has a much higher ionic conductivity at an intermediate temperature than the more popular electrolyte material of yttria-stabilized zirconia (YSZ), is regarded as one of the more hopeful candidates for the intermediate temperature SOFCs electrolyte. In this paper, we develop a simple, rapid and cost-effective method, which is based on dry pressing and powder spray coating process. The spray dry co-pressing method is developed to prepare a dense bilayer electrolyte thin film for anode-supported SOFCs. The dry pressing method is a simple, reproducible, and very cost effective process. This technique has been widely used in the laboratory and industry to produce a thick substrate. However, it is very difficult to prepare a thin electrolyte by the dry pressing method because of the difficulty in controlling the uniform distribution of electrolyte powder on a substrate surface. Consequently, the powder spray coating process is employed in this study. The powder spray process is a simple and cost-effective method with a thickness of less than 10μm.

3.1.1 Literature survey

Many researchers have reported various processes of fabrication for intermediate SOFCs based on a thin-film electrolyte doped ceria such as tape casting[7], screen printing[8,9], dry pressing[10,11], spray coating[12,13], spin coating [3], slurry coating[14], and sol-gel[15]. However, the reduction of ceria from Ce4+ to Ce3+ in a reducing atmosphere will increase electronic conductivity, which decreases the open-circuit voltage (OCV) of the cell. Furthermore, reduction of ceria also causes lattice expansion of the ceria electrolyte at the anode side. One approach proposed to prevent the OCV drop and to improve the chemical and mechanical stability of doped ceria electrolytes in reducing atmospheres is to coat thin YSZ film on the anode side of a doped ceria electrolyte. The YSZ/GDC bilayer electrolyte can be a barrier of a doped ceria electrolyte from a reducing mood.

Since the ionic conductivity of YSZ is lower than gadolinia-doped ceria (GDC) at an intermediate temperature, the YSZ film as an electronic and hydrogen blocking layer should be adequately thin to minimize its contribution to total electrolyte resistance. Therefore, techniques such as chemical vapor deposition (CVD) [16], pulsed laser deposition (PLD) [17], RF magnetron sputtering [18], and wet-ceramic process [19] have been developed to deposit a thin film of YSZ on doped ceria electrolyte.

3.2. Research Methodology

GDC (Gd0.1Ce0.9O1.95, Nextech, USA) and 8mol% YSZ (Y2O3/ZrO2, Nextech, USA) commercial powders were used as an electrolyte. Commercial NiO (60 wt %) and GDC (40 wt %) powder were mixed and ground with alcohol and a little amount of polyvinyl butyral (PVB) for two hours. Afterward, the mixture was dried and screened through a 110-mesh sieve. For the preparation of the green body, the NiO and GDC mixed powder was first pressed under 60 MPa into a substrate in a SKD11 steel die. Then, the YSZ slurry was mixed properly with iso-propanol and was spray coated onto a NiO/GDC substrate that is in steel die. Finally, the GDC powder was added onto the YSZ layer through a sieve and co-pressed at 80 MPa to form a green assembly. The green assembly was subsequently co-fired at 1400°C for five hours in air. A dense, crack-free and well-bonded GDC-YSZ bilayer electrolyte-anode assembly was obtained.

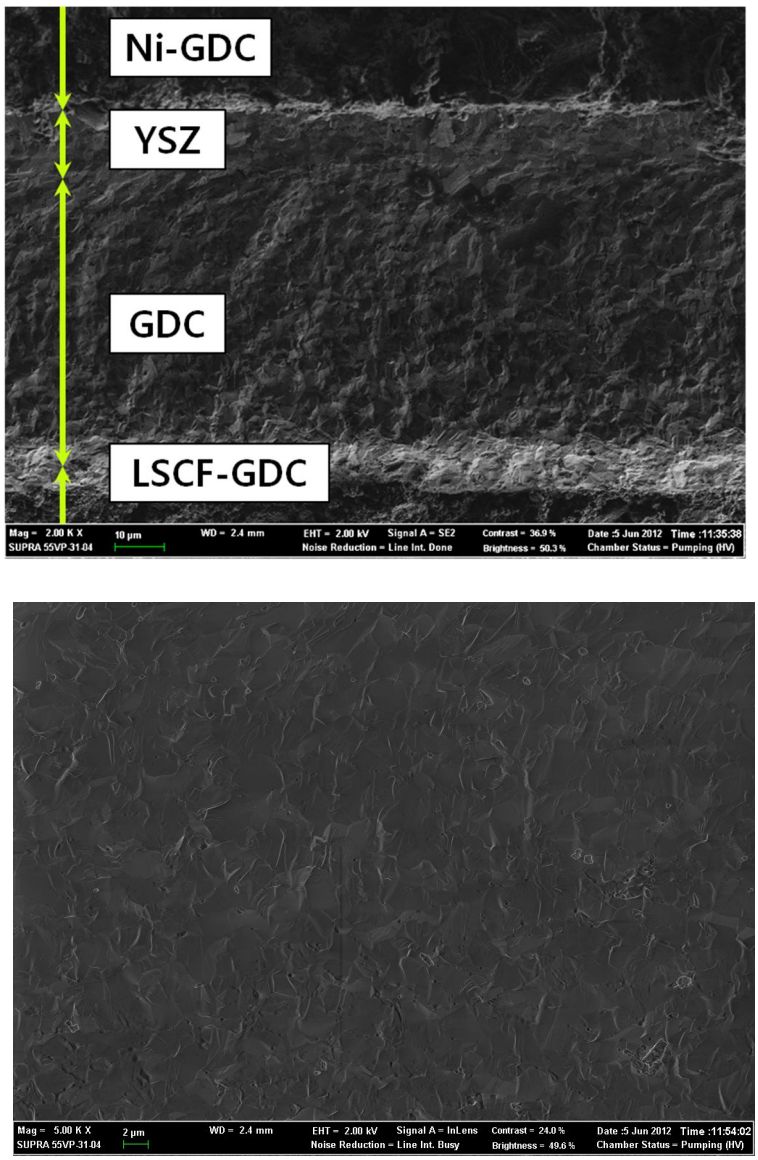

Figure 3.1. (a) Scanning electron microscopy of cross-section of a YSZ/GDC bilayer electrolyte film on a anode substrate. (b) morphology of GDC electrolyte plane

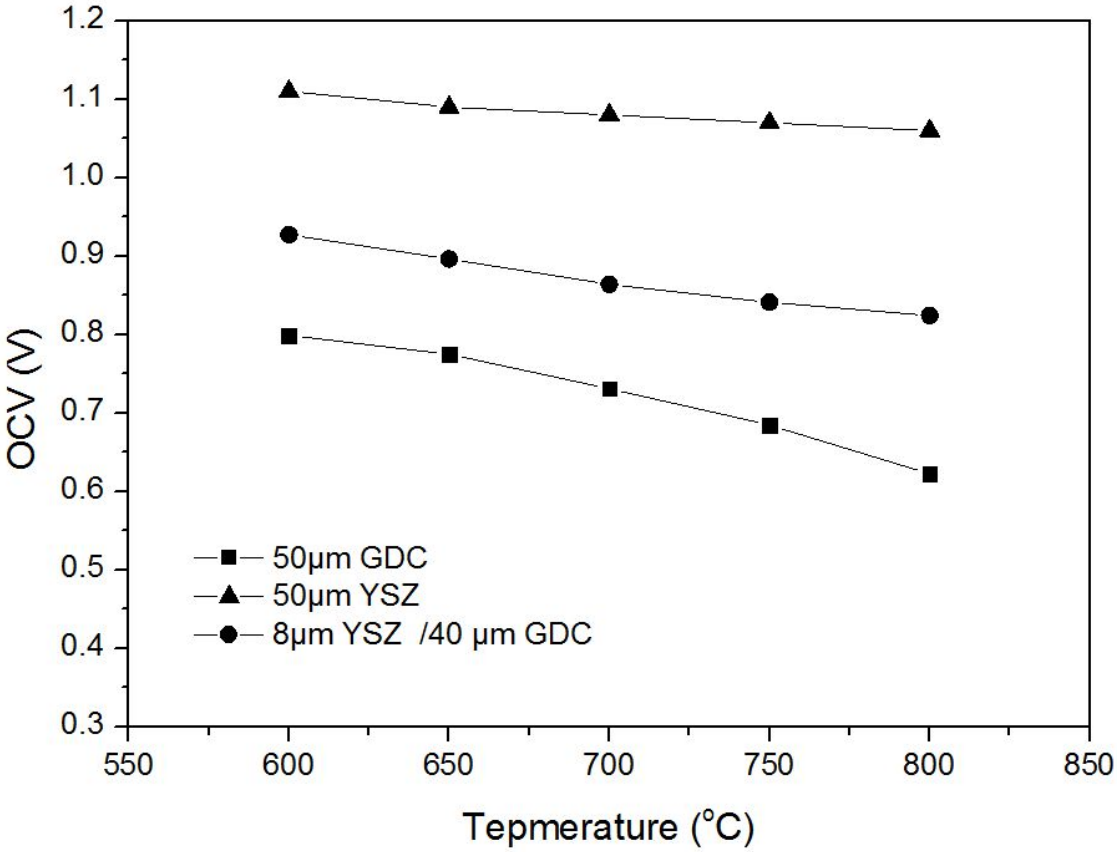

Figure.3.2. Measured OCV vs temperature for single cells with 50 μm GDC monolayer electrolyte, 50 μm YSZ monolayer electrolyte, and 8μm YSZ/ 40μm GDC bilayer electrolyte, respectively.

The diameters of the green pellets and sintered pellets were 25 and 22 mm, respectively. The thickness of the YSZ and GDC layers was controlled by the spray time and amount of powder, respectively. The total thickness of the electrolyte-anode substrate assembly was 2mm. The porous cathode was prepared using a mixture of 60 wt % strontium-doped lanthanum cobaltite ferrite (La0.6Sr0.4Co0.8Fe02O3) and 40 wt % GDC. The mixture was applied by screen printing and was fired at 900°C for two hours in air. The area of the cathode was 0.5 cm2.

The single cell was sealed using a gold ring on one end of an INCONEL jig. The surface of outer side of gold ring was coated ceramic sealant (Aremco 503) to prevent leakage of hydrogen. Platinum meshes were used as current collectors. The single cell was pressured by a bolt of jig. After the in situ reduction of the NiO anode in H_2 for several hours, the performances of the cell were measured at various temperatures from 600 to 800°C. Hydrogen passed over the anode at a flow rate of 100 sccm with 3% H_2O, and air flowed over the cathode surface at a flow rate of 100 sccm. The impedances were measured typically in the frequency range from 0.05 Hz to 50 kHz under open-circuit conditions using a Solartron 1287 potentiostat and 1260 frequency-response analyzer. The tested cell was fractured and examined by a scanning electron microscopy (SEM). The SEM observation was performed on a scanning electron microscope (SUPRA 55VP, Carl Zeiss).

3.3. Results

The YSZ layer is required to be dense and crack-free to prevent exposure of the GDC layer to the hydrogen. This effectively serves as an electronic blocking layer. In addition, the YSZ film is required to be suitably thin to minimize the ohmic resistance of the electrolyte. Figures 3.1(a) and 3.1(b) show cross-sectional and surface micrographs of the YSZ/GDC bilayer electrolyte film on a reduced Ni–YSZ anode substrate. Total thickness of the YSZ/GDC bilayer electrolyte is about 50μm, which consists of a 8μm YSZ layer and a 40μm GDC layer.

In addition, a uniform film YSZ is joined well by a NiO-GDC anode substrate. The YSZ film is also densely sintered without any cracks and pores. Finally, the GDC film is well bonded to the LSCF cathode. This SEM measurement was measured for several hours after the electrochemical operations. This suggests that the cell by dry co-pressing process verifies that the YSZ/GDC bonding is very stable even under the operation of the fuel cell. It also indicates that the two electrolyte layers and anode layer are thermo-mechanically matched during the high temperature co-sintering process. The interfacial diffusion during the high-temperature co-sintering (1100C ~) that causes the formation of solid solutions at the interface of YSZ and GDC layers. Zhou et al. [65] investigated the thermal expansion behaviour of $(GDC)_x(YSZ)_{1-x}$ solid solutions in detail and found that the TEC of the $(GDC)_x(YSZ)_{1-x}$ system increases with increasing GDC fraction from that of pure YSZ ($\sim 10.7\times10^{-6}\ K^{-1}$) to that of pure GDC ($\sim 13.2\times10^{-6}\ K^{-1}$). This behavior implies that the formation of solid solutions from YSZ/GDC diffusion interface will create a functional graded layer between the YSZ and GDC layers, which would help to reduce the thermo-mechanical breakdown of a fuel cell with the YSZ/GDC bilayer electrolyte.

The (GDC)x(YSZ)1−x layer has low ionic conductivity which increase ohmic overvoltage, but it has positive effect to mechanical stability and open circuit voltage. So, total performance is improved.

With respect to the YSZ/GDC bilayer electrolyte cell by dry co-pressing quality, a GDC single electrolyte cell and YSZ single electrolyte cell were prepared using a LSCF-GDC (50:50 by weight) composite material as the cathode. Subsequently, the single electrolyte cells were electrochemically tested in humidified hydrogen (3 vol. % H_2O)/air (20% O_2; 80% N_2) at a temperature range of 600 to 800°C. The electrolyte thickness for both single cells was about 50μm, and thus, the same electrolyte thickness of the total YSZ/GDC bilayer cell. Figure 3.2 shows the measurement of the OCVs of the GDC single layer cell, YSZ single layer cell, and the YSZ/GDC bilayer cell. The OCVs of the YSZ/GDC bilayer cell is 1.09, 1.07, 1.042, 0.98 and 0.94V at 600, 650, 700, 750, and 800°C, respectively. The OCVs of the YSZ/GDC is more enhanced than the OCVs of the GDC single layer cell. However, it is lower than the OCVs of the YSZ single cell at high temperature range. Therefore, the YSZ layer in the YSZ/GDC bi-layer cell prevents reduction of the GDC electrolyte at low and intermediate temperature. .

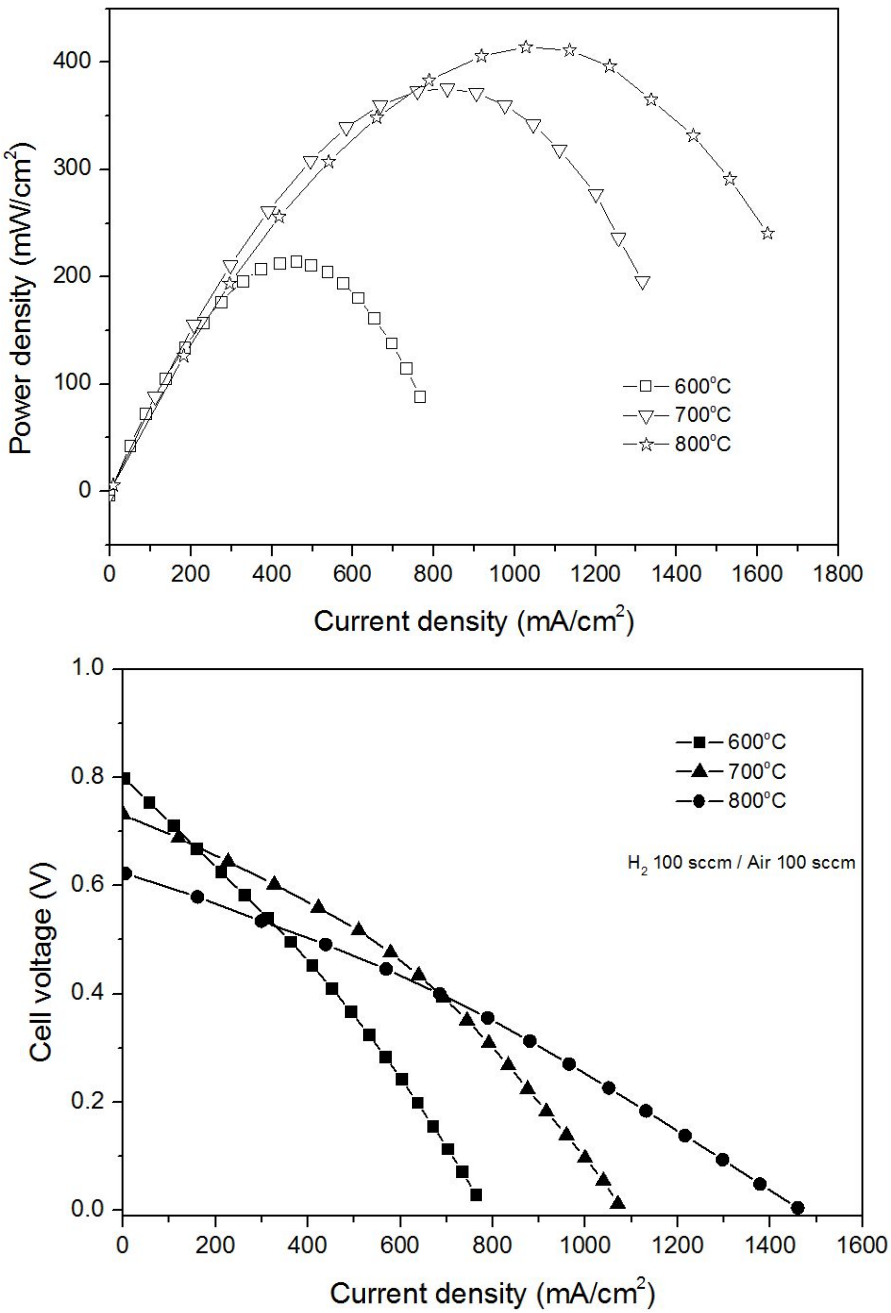

Figure. 3.3 (a) Cell voltage and (b) power density as function of current density of a YSZ (8 μm)/GDC (40 μm) bilayer electrolyte cell measured between 600 and 800 °C in humidified hydrogen and open air.

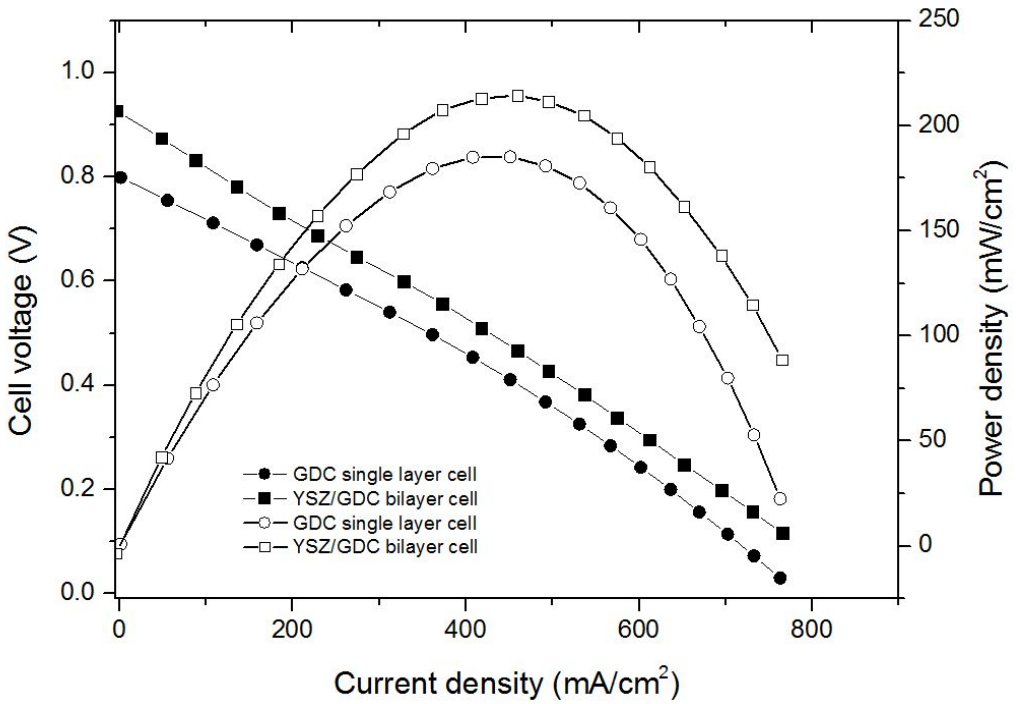

Fig. 3.4 Cell voltage and power density vs. current density of a YSZ (8 μm)/GDC (40 μm) bilayer electrolyte cell measured 600 ◦C in humidified hydrogen and open air.

The current-power density and current-voltage characteristics of the YSZ/GDC bilayer electrolyte cell were measured between 600 to 800°C. Figure 3.3(b) shows that the maximum power densities of the YSZ/GDC bilayer electrolyte cell are 208, 403, 481mW/cm^2 at the temperatures of 600, 700, and 800°C, respectively. For the purpose of comparison, the current-power density and current-voltage characteristics of the GDC single layer cell was measured in the same manner. Figure 3.4 shows the characteristics measurement of the GDC single layer electrolyte cell and YSZ/GDC bilyaer electrolyte cell at 600°C. The maximum power density of the GDC single layer cell is 180mW/cm^2. The result demonstrates that the peak performance of the YSZ/GDC bilayer cell is higher than one of the GDC single cells because of higher OCVs. Figure 3.5 shows an electrochemical impedance spectroscopy (EIS) result regarding the GDC single electrolyte cell and YSZ/GDC bilayer electrolyte cell. The YSZ/GDC bilayer electrolyte cell has lower ohmic resistance than one of the GDC single layer electrolyte-cells. Therefore, the YSZ film layer in the YSZ/GDC electrolyte prevents reduction of the ceria electrolyte, even though the YSZ film has low ionic conductivity in an intermediate temperature, Thus, the results demonstrate that the micron thickness of the YSZ film is sufficiently effective.

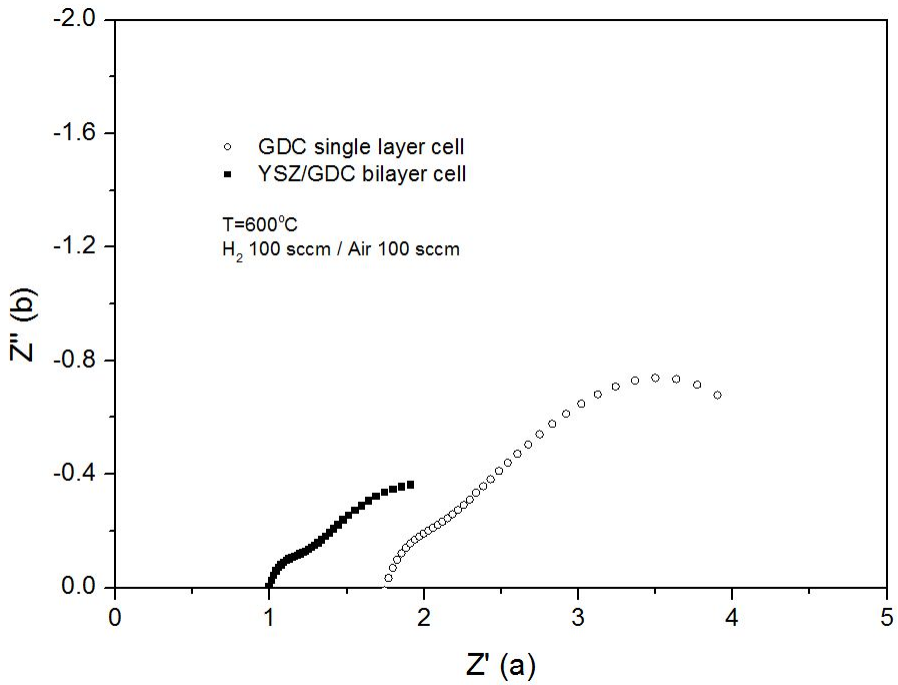

Fig. 3.5 Result of electrochemical impedance spectroscopy of GDC single electrolyte cell and YSZ/GDC bilayer electrolyte cell, 600°C

3.4 Conclusion

The spray dry co-pressing method was developed as a simple, rapid and cost-effective method. An anode-supported SOFC single cell with YSZ-GDC bilayer electrolytes, Ni-GDC cermet as an anode, and $La_{0.6}Sr_{0.4}Co_{0.2}Fe_{0.8}O_3$ (LSCF)-GDC composite as a cathode was fabricated. The SOFCs based on YSZ-GDC bilayer electrolytes were tested from 600 to 800°C with hydrogen, which contained 3% water as fuel and air as an oxidant. Maximum power densities of 218 and 421 mW/cm^2 were achieved at 600 and 800°C, respectively. The OCV was 0.91 and 0.68 V at 600 and 800°C, respectively. The results suggest that the spray dry co-pressing technique is a practical process to prepare bilayered dense electrolyte films for low-temperature SOFC applications. In addition, the findings suggest that for a thin-film cell with YSZ/GDC bilayer electrolytes, the reactions between YSZ and cathode material at high temperatures can be prevented. However, the electronic conductivity of a GDC electrolyte is blocked by the YSZ layer. In this study, we did not employ sufficiently porous anode substrate which can offer low concentration and activation overvoltage. So, we will employ anode pore-former for increasing power density, in future study.

Chapter 4. Anode functional layer for porous anode substrate

4.1 Introduction

In previous experiment, we used a dense anode substrate material. Using dense substances, cell fabrication and operation of the mechanical stability can be improved. However, dense anode substrate makes it difficult for low and medium on the permeation of hydrogen in the area. This is why limit the performance of the cell in the intermediate temperature range.

Since that point, it is necessary that make cell using porous anode substrate. There is a performance benefit using porous anode substrate. In Contrary, it makes mechanical, structural stability degraded. In this chapter, we suggest advantages, shortcomings and propose solutions of the cell.

4.2 Porous anode substrate cell

4.2.1 Porous anode substrate cell fabrication

In order to confirm improving the performance and mechanical strength of porous anode substrate cell, we were made porous anode substrate bi-layer electrolyte cell. We fabricated test cell using cold press process mentioned previously. We controlled whole compaction process same as previous study, except using anode substrate material with NiGDC cermet powder adding PMMA powder.

The PMMA material is one of the popular pore former materials like carbon powder. In this study, we did not consider optimum pore-size and pore-ratio. We employed 5um PMMA size that generally used as pore former. The ratio is 10wt% with NiGDC cermet. Powder production method is that mixed cermet and PMMA powder materials with ethanol vehicle and stirring 2 hours. And then it was dried at room temperature

4.2.1 Cell fabrication

The fabrication process is identical with previous bi-layer cell fabrication process except preparing anode substrate powder.

GDC (Gd0.1Ce0.9O1.95, Nextech, USA) and 8mol% YSZ (Y2O3/ZrO2, Nextech, USA) commercial powders were used as an electrolyte. To make porous anode substrate, PMMA(JT. Baker) was prepared as pore former.

PMMA(JT Baker), NiO (60 wt %) and GDC (40 wt %) powder were mixed and ground with alcohol and a little amount of polyvinyl butyral (PVB) for two hours. Afterward, the mixture was dried and screened through a 110-mesh sieve. For the preparation of the green body, the mixed porous substrate powder was first pressed under 60 MPa into a substrate in a SKD11 steel die. Then, the YSZ slurry was mixed properly with iso-propanol and was spray coated onto a NiO/GDC substrate that is in steel die. Finally, the GDC powder was added onto the YSZ layer through a sieve and co-pressed at 80 MPa to form a green assembly. The green assembly was subsequently co-fired at 600°C for 1 hour to burn. And, It was co-sintered at 1400°C for five hours in air. A porous substrate and dense elecrolyte, crack-free and well-bonded GDC-YSZ bilayer electrolyte-anode assembly was obtained.

4.2.2 Cell test result

There were significant differences results in using porous anode substrate cell with PMMA and dense substrate cell. We had expected performance increasing due to be reduced concentration loss. However, there were few influences from concentration loss between dense substrate cell and porous substrate cell. But, it is reduced that activation rate 5 hour to 1hour. Moreover, high porosity affects to decrease activation loss significantly. Accordingly, we obtained higher performance of porous cell than one of dense cell at high temperature ranges. At 800^{o}C, we obtained 620mW/cm^{2} power density, and at 700^{o}C, it was shown 460mW/cm^{2} power density.

Nevertheless, the pore of anode substrate caused reducing mechanical stability. Although reduced activation time affected positive effect real cell operation, but it caused fast degradation issue. These are considered that differences of thermal expansion coefficient and weak bonding between anode substrate and electrolyte inter-surface are that reasons.

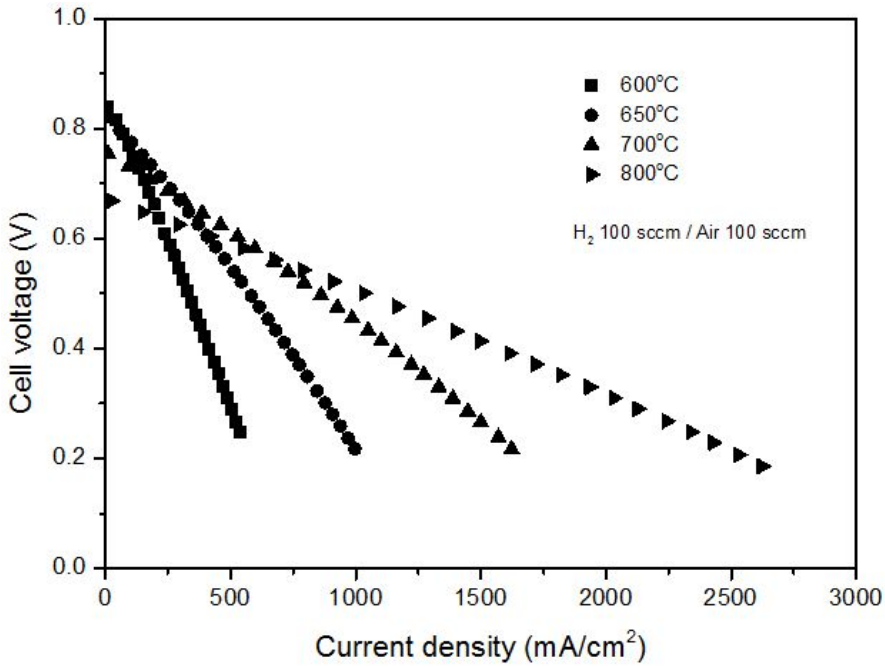

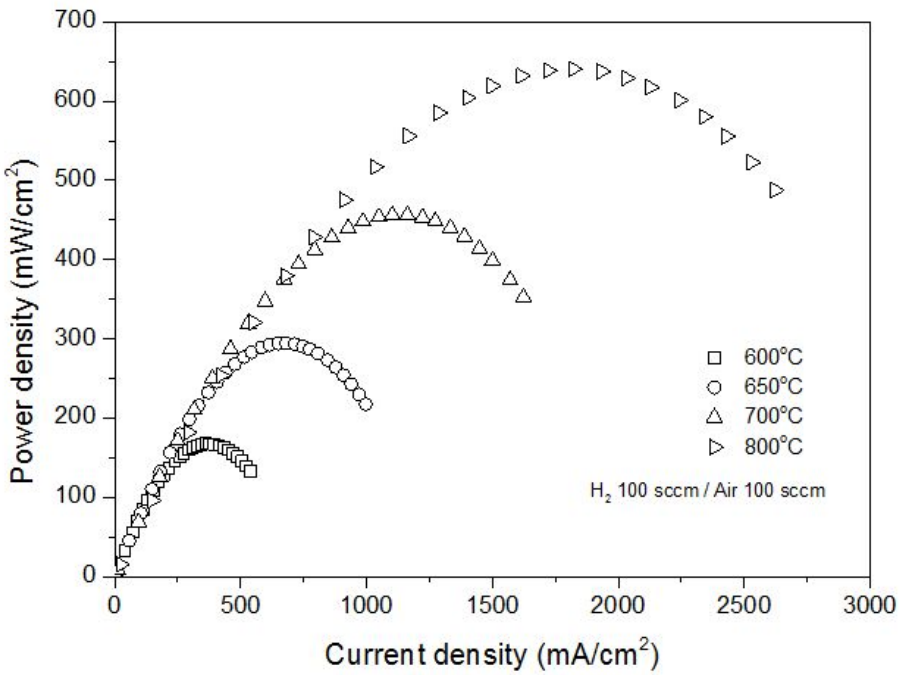

Figure 4.1 IV and power density of PMMA porous substrate bi-layer electrolyte cell

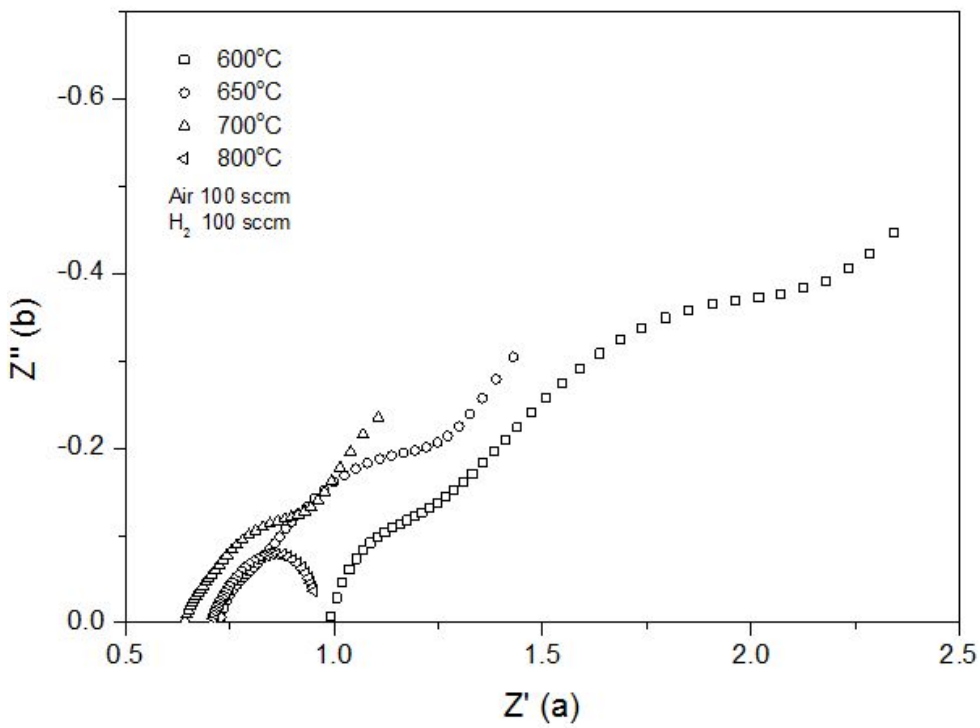

Figure 4.2 EIS reslut of PMMA porous substrate bi-layer electrolyte cell

4.3 Anode functional layer cell

4.3.1 Fabrication

We have added the anode functional layer to makeup the shortcomings of previous porous anode substrate cell. The conventional dense NiGDC powder was used as the anode functional layer material. This anode functional layer was expected increase mechanical stability and electrochemical performance.

GDC ($Gd_{0.1}Ce_{0.9}O_{1.95}$, Nextech, USA) and 8mol% YSZ ($Y2O_3/ZrO_2$, Nextech, USA) commercial powders were used as an electrolyte. Commercial NiO (54 wt %), GDC (36 wt %) and PMMA (10 wt %, Sigma Aldrich) powder were mixed and ground with alcohol and a little amount of polyvinyl butyral (PVB) for two hours. Afterward, the mixture was dried and screened through 110-mesh sieve. For the preparation of the green body, the NiO-GDC and PMMA mixed powder (or NiO-GDC powder only) was first pressed under 60 MPa into a substrate in a SKD11 steel die. The anode functional layer material was mixed properly with ethanol and was spray coated onto anode substrate green body. Then, the YSZ slurry was mixed properly with iso-propanol and was spray coated onto a NiO/GDC substrate or anode functional layer that is in steel die. Finally, the GDC powder was added onto the YSZ layer through a sieve and co-pressed at 80 MPa to form a green assembly. The green assembly was subsequently co-fired at 1400°C for five hours in air.

The porous cathode was prepared using a mixture of 60 wt % strontium-doped lanthanum cobaltite ferrite ($La_{0.6}Sr_{0.4}Co_{0.8}Fe0_2O_3$) and 40 wt% GDC. The mixture was applied by screen printing and was fired at 900°C for two hours in air. The area of the cathode was 0.5 cm2.

Cells were made in the method a total of five. The Anode substrate material was employed dense NiGDC. In 2, 3, 4 and 5 times, we used NiGDC-PMMA. Electrolyte used YSZ / GDC of all cells.

The problem with YSZ / GDC electrolyte bilayer, layer thin YSZGDC substance is generated by the diffusion reaction between the YSZ and GDC hot new view, the ion conductivity of the electrolyte is lowered occurs. Despite these shortcomings, to obtain structural stability GDC electrolytes by the role of YSZ is I prevent the reaction with H_2 at low oxygen partial pressure of GDC, is in performance due to increase in the OCV lead to improvement .

We prepare a cell having a thickness of four to confirm the effect of the thickness of anode functional layer. Distinction between the anode functional layer and Anode substrate is because it is not easy, and was produced by changing the weight of NIGDC using the functional layer. I was adjusted to the amount of solution in the amount NIGDC + ethyl-cellulose + ethanol of anode functional layer of the cell was produced. The amount of solution used during fabrication of each cell was used and 1, 4, 8 and 12mg. In consideration of the size of the cell density and the NIGDC, was calculated by estimating the thickness estimation. After sintering process, the thickness of the anode functional layer is calculated 6,10,14 and 19 microns respectively.

Table 4.1 Various approach for fabrication of anode functional layer

Cell number	Anode substrate	Anode fuctional layer	
1	NiGDC		
2	NiGDC-PMMA		
3	NiGDC-PMMA	NiGDC Spray	Sintering failure
4	NiGDC-PMMA	NiGDC Sieve	Pressing failure
5	NiGDC-PMMA	NiGDC+Ethyl cellulose(1.5%) spray	

Table 4.2 Thickness of Anode functional layer

Cell number	Anode substrate	Thickness of anode fuctional layer(micro meter)
5-1	NiGDC- PMMA	6
5-2	NiGDC-PMMA	10
5-3	NiGDC-PMMA	14
5-4	NiGDC-PMMA	19
2	NiGDC-PMMA	none

4.3.2 Experimental

The single cell was sealed using a gold ring on one end of an INCONEL jig. The surface of outer side of gold ring was coated ceramic sealant (Aremco 503) to prevent leakage of hydrogen. Platinum meshes were used as current collectors. The single cell was pressured by a bolt of jig. After the in situ reduction of the NiO anode in H_2 for several hours, the performances of the cell were measured at various temperatures from 600 to 800°C. Hydrogen passed over the anode at a flow rate of 100 sccm with 3% H_2O, and air flowed over the cathode surface at a flow rate of 100 sccm. The impedances were measured typically in the frequency range from 0.05 Hz to 50 kHz under open-circuit conditions using a Solartron 1287 potentiostat and Solartron 1260 frequency-response analyzer. The tested cell was fractured and examined by a scanning electron microscopy (SEM). The SEM observation was performed on a scanning electron microscope (SUPRA 55VP, Carl Zeiss).

4.3.3 Result

For a porous substrate and dense substrate, we were confirmed whether with what features. For a porous substrate, fast activation and at the same time advances, it was confirmed that through rapid deterioration process, performance is degraded rapidly.

It was produced in a variety of ways the anode functional layer in order to improve the mechanical stability of Porous substrate. Method using a sieve general, failed made by delamination or crack during pressing. In addition, Ni - how you spray coating is made with slurry by mixing the ethanol and GDC, failed to sintering progress. To prepare a cell with certainty in a way that was added Ethyl cellulose (1.5 %) in ethanol solution and GDC, was spray coating - Ni. The reason is because it is present in the form of powder and electrolytes substrate, and has a sufficient adhesion during the sintering process of adding Ethyl cellulose of the polymeric adhesive component.

The experimental results it is possible to see the effect of anode functional layer. For porous substrate cell anode functional layer is added, shows the performance slightly higher than the porous substrate cell for which there is no functional layer. I show higher performance than the dense substrate cell two cells. Looking at the pictures after the experiment, in the case of the Anode functional layer cell, it can be confirmed that the crack and deterioration of the cell much less compared to the cell functional layer is not present.

It is possible to verify the performance and characteristics corresponding to the thickness of the functional layer. The thickness of the functional layer is 6, 10, 14 and 19um respectively. For all cells, it is possible to confirm that the

performance improvement of some present as compared to cells without the functional layer. However, as the thickness of the functional layer is thick, it's small, but performance degradation was confirmed. This, we can be considered to be due to the electrical resistance of the functional layer. We were considered that due to limitations in the thickness of the layer when the cold press process, the functional layer of 5 micrometers is the most advantageous in terms of performance. I was able to see how the stability increases as the functional layer becomes thick overall.

In this experiment, to check additional functional layer whether improve the performance electrochemically, and it was not easy. For non-functional layer is compared, cracks and deterioration of the cell occurs in the early hours, is not withdrawn optimal performance, the conclusion that the functional layer influences the performance improvement electrochemically whereby it is not easy. However, make sure that you provide stability and behavior mechanical stability of the structure of dry-pressed these, the presence of the functional layer , useful for the survival of the cell, making the cell structure porous like this that when you, functional layer that will play a role of a buffer is absolutely necessary could be confirmed.

In case of 19um AFL cell, it shows similar IV curve to dense substrate bi-layer cell (Figure 4.5). It means thick anode functional layer works as dominant anode component that affects to conductivity triple boundary layer. The dense anode has lack of porosity that has advantage of concentration of hydrogen leads to drop performance rather than thinner anode functional layer cell.

Figure 4.6 shows that the trend of thickness of anode functional layer affection. In this study, optimal thickness of anode functional layer is 10um. Thicker AFL cell has performance drop cause of its dense properties, and thinner AFL cell has not

enough AFL effect cause of lack of capacity of thermal matching and dense triple boundary layer effect. The optimal thickness is considered flexible. It is depending on anode material size, density, total thickness, etc. So, in this study, we established there's optimal thickness of AFL(10um) of our condition, and we suggested some trend of preparation of cell fabrication .

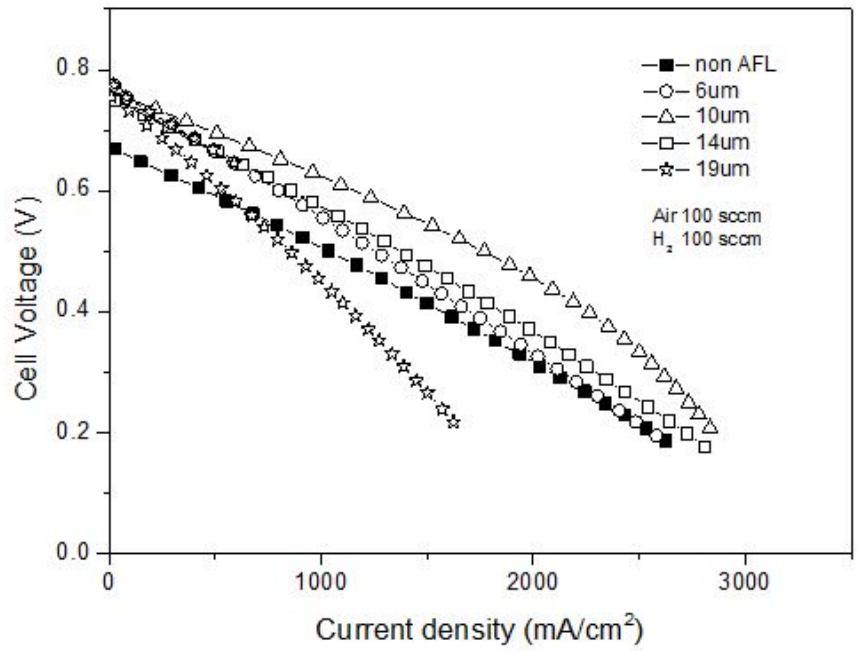

Figure 4.3 IV performance curve in various thickness of anode functional layer

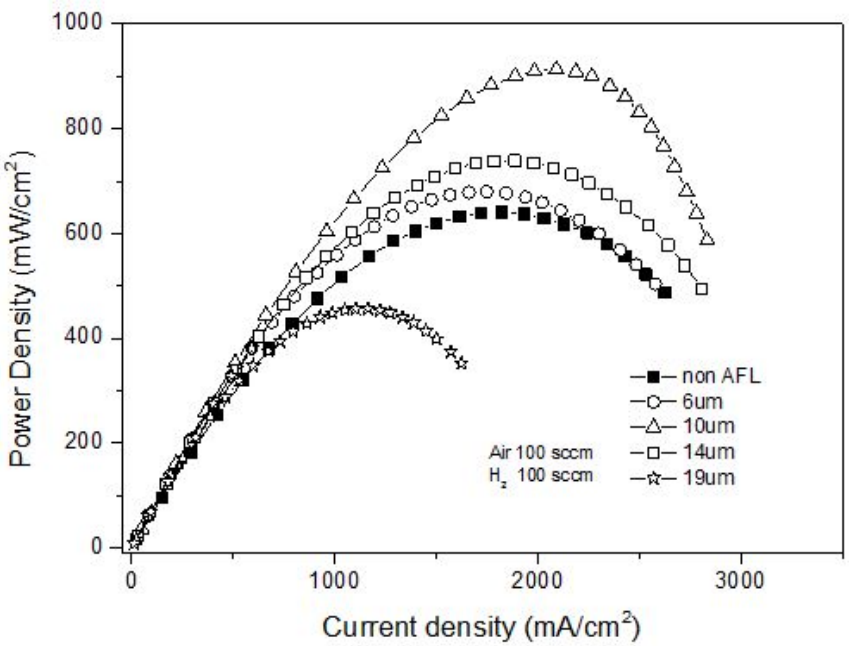

Figure 4.4 Power density in various thickness of anode functional layer

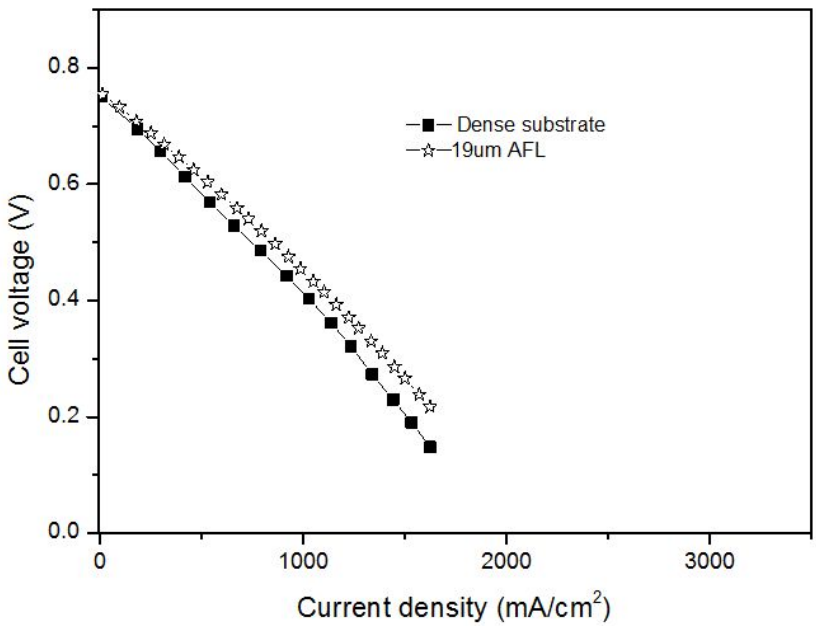

Figure 4.5 Similarity of IV curve of dense anode substrate cell and thick anode functional layer cell

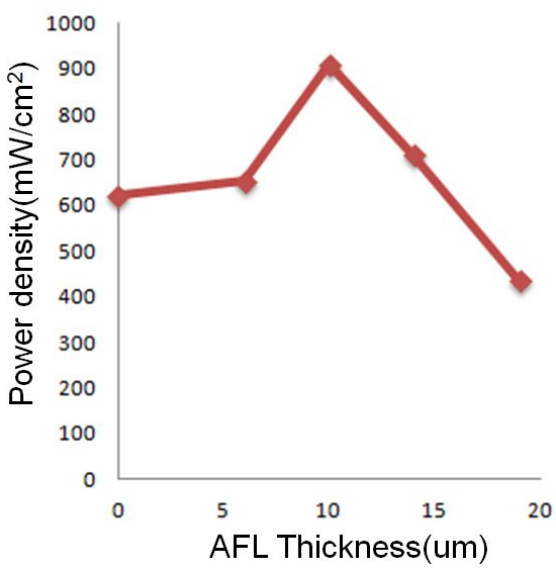

Figure 4.6 Peak power density of various thickness of anode functional layer

4.3.4 Discussion

Through this study , when using a anode electrode substrate with porous in the fabrication of the anode electrode-supported solid oxide fuel cell using a dry pressing process that is a process efficient and economical, and mechanical stability due to the addition of the functional layer of the cathode side to confirm that it was a very important part.

In order to fabricate at the anode electrode-supported solid oxide fuel cell using a dry pressing step, to improve performance, so that it requires a sufficient pore portions of the anode support. The dry-pressing process, for sintering the ball anode support and the electrolyte, in order to create enough pin hole in the anode electrode substrate used is essential to hydrocarbons. In order to compensate for expansion due to thermal stress and the anode electrode substrate and the electrolyte due to the use of these hydrocarbons, the functional layer of the anode electrode is always required.

In this study, we confirmed the manufacturing process of optimal anode functional layer in the anode substrate and porous. It is also possible to test the cell using the anode functional layer, it was also confirmed the mechanical stability of the cell. Anode functional layer was also confirmed that a certain part contributes to the improved performance of the cell.

It was tested by manufacturing a cell using the functional layer having a thickness of four to confirm the characteristic according to the thickness of the functional layer, to check the performance changes. As a result, it was confirmed that in accordance with the thickness, having different properties, respectively. We were significantly improved for performance and optimum stability in 10 micro meters anode functional cell.

It is expected that if the research on examining the performance point of optimal according to the porosity of the anode substrate are performed simultaneously, and be able to derive the result of the optimum thickness of the functional layer in its optimum substrate porosity more conditions.

Chapter 5. Numerical analysis of behavior of fabrication process by finite element method

5.1 Introduction

There is the difference between cold press process and a common process in producing cell. In conventional wet ceramic process and thin film deposition process, TCE between anode substrate and film is a mechanical strength issue. However, in the cold press process, compacting ceramic powder is one of the most important processes. The feasibility of cell is most important issue in the cold press process.

The powder compaction is carried out using steel die. In this uni-axial compression, knowing powder behavior is necessary components to fabricate mechanically stable cell. In addition, if we control the residual stresses remain minimal, it is possible that we minimize influence of sintering process which is stepped after compaction.

In this study, we approached compaction issue using COMSOL multi-physics.

5.2 Geometric description

Figure 5.1 schematically shows the 2D axisymmetric model of a substrate of SOFC fuel cell which was constructed using COMSOL model builder. To simplify the model, we calculated the 2D axisymmetric of the unit cell. The model has main domain part which is consist of anode substrate powder materials and 1 or 2 layers domain which are consist of electrolyte materials.

We modeled cell dimension of anode substrate and electrolyte thickness ratio little bit differently due to mapping problems in COMSOL multiphysics.The geometry of cell was constructed as shown in Table 5.1.The anode substrate domain, we modeled the thickness of 30mm, diameter 26mm the same as were made real cell. The electrolyte layer, the thickness of YSZ and GDC, respectively 100, 300 um in modeling was performed.

Table 5.1 Dimension and global parameter of the substrate model

Parameter	Anode Substrate	YSZ electrolyte	GDC electrolyte
Height	30mm	100um	300um
Diameter	26mm		
Compression	100MPa	100MPa	100MPa

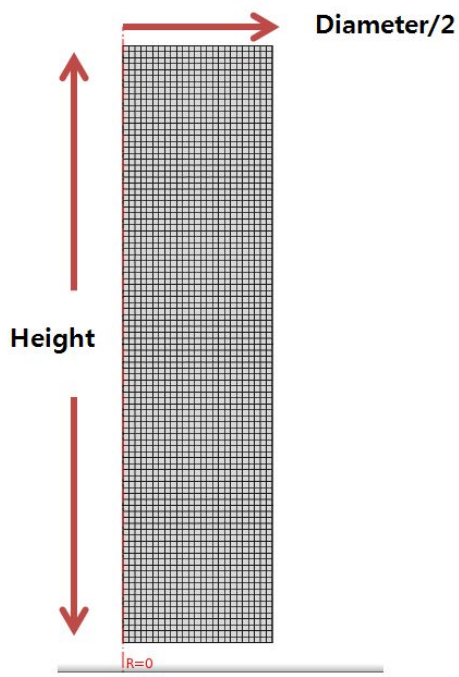

Figure 5.1 Schematic diagram of the substrate model

5.3 Model description

The complete mathematical statement of this model consists of the following. In this approach, the powder is considered as a porous media and is characterised by overall parameters such as cohesion, global interparticle friction and mechanical properties such as the Young's modulus and the Poisson ratio, which can depend on density during the compaction. In the present work, a Drucker–Prager Cap model is used to analyse the strain, stress and relative density changes in a ceramic powder during the compression.

The yield surface of this model consists of a linear slope describing failure under shear stresses with superimposed hydrostatic pressure, and an elliptical cap forming the boundary of the yield surface in direction of the hydrostatic axis, (Figure. 5.2). The cap yield surface is given by

$$\varphi = \sqrt{(p - p_a)^2 + (\frac{Rt}{1 + \alpha - \alpha/cos\beta})^2} - R(d + p_a tan\beta) = 0 \quad (5.1)$$

where p is the hydrostatic stress, and t is a combination of the second and the third stress invariant. It coincides with the second invariant if the third invariant is neglected. tan B is the slope of the shear failure line, d is a parameter describing the amount of cohesion between the particles, R describes the shape of the cap, and Q describes a transition surface between cap and failure line; p_b is a hardening parameter, and pa is given by

$$p_a = \frac{p_b - R_d}{Rtan\beta + 1} \quad (5.2)$$

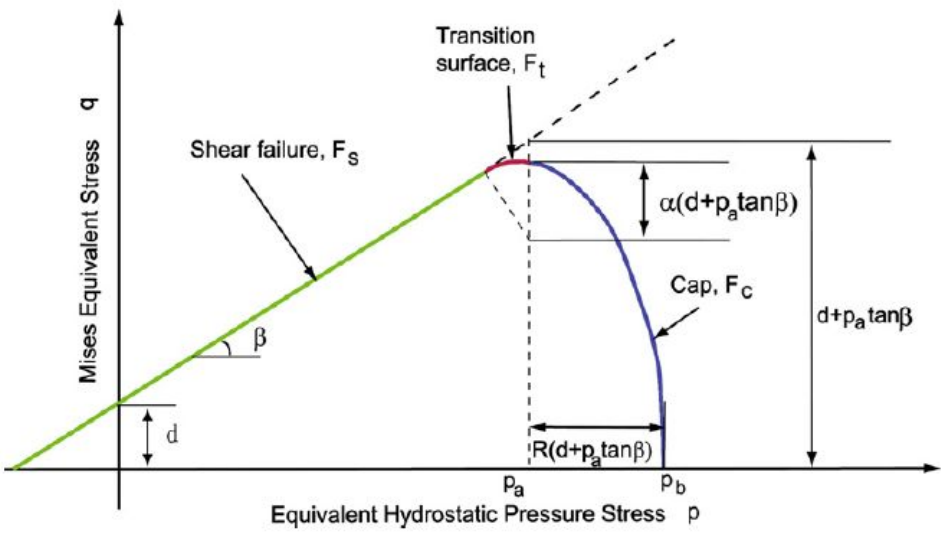

Figure 5.2. Drucker-Prager Cap model: yield surface in the p-q plane.

5.4 Analysis result

We carried out finite element modeling.which is applied Drucker-Prager cap model using COMSOL multi-physics. We can see the result value Surface von mise stress in COMSOL. As compared these surface von mise stress with the material yield criterion stress, we can predict phenomenon of cell failure that may occur during the compaction process.

We were used known properties of GDC, Ni, NiGDC and YSZ material. [77,78,79] The properties are Young's modulus, Poisson ratio, density and etc. (Table 5.2) Using these properties, we obtained surface von Mise stress by COMSOL multi-physics.

Anode substrate material was modeled and calculated based on NiGDC dense powder substrate properties. The known properties were NiO powder, GDC powder and YSZ powder, so we assumed mixed powder properties using interpolation and extrapolation by wt% ratio. In addition, we assumed properties about different properties from powder size, using same manner with known GDC powder and NiO powder properties.

We used a layer domain as electrolyte material layer. We employed previously known properties of GDC powder and YSZ powder for modeling and calcuating[77,78,79].

As shown Figure 5.3, it is result of 3D FEA analysis. As you can see, both of GDC and YSZ powder, we can confirm that smaller powder size affects to represent a higher stress. In addition, in the case of YSZ powder present higher stress rather than the case of GDC powder. This means the difference of material properties between GDC and NiGDC is smaller than difference of material

properties between YSZ and NiGDC.

The surface von mise stress is 1.17E7 at 0.5um GDC, 1.08E7 at 3.5um GDC, 2.1E7 at 0.53um YSZ and 1.29E7 at 5.7um YSZ, respectively.

Table 5.2 Properties of materials for FEM modeling

	YSZ-m	GDC-m	YSZ	GDC	NiO	NiGDC
Full density	6.08	7.04	6.08	7.04	6.828	6.913
Particle siz	0.53	0.5	5.7	3.5	4	3.8
β	54.3°	54.3°	54.3°	54.3°	54.3°	54.3°
α	0.03	0.03	0.03	0.03	0.03	0.03
E	206GPa	187GP	190GPa	187GP	205GPa	198
ν	0.31	0.324	0.31	0.324	0.3	0.31

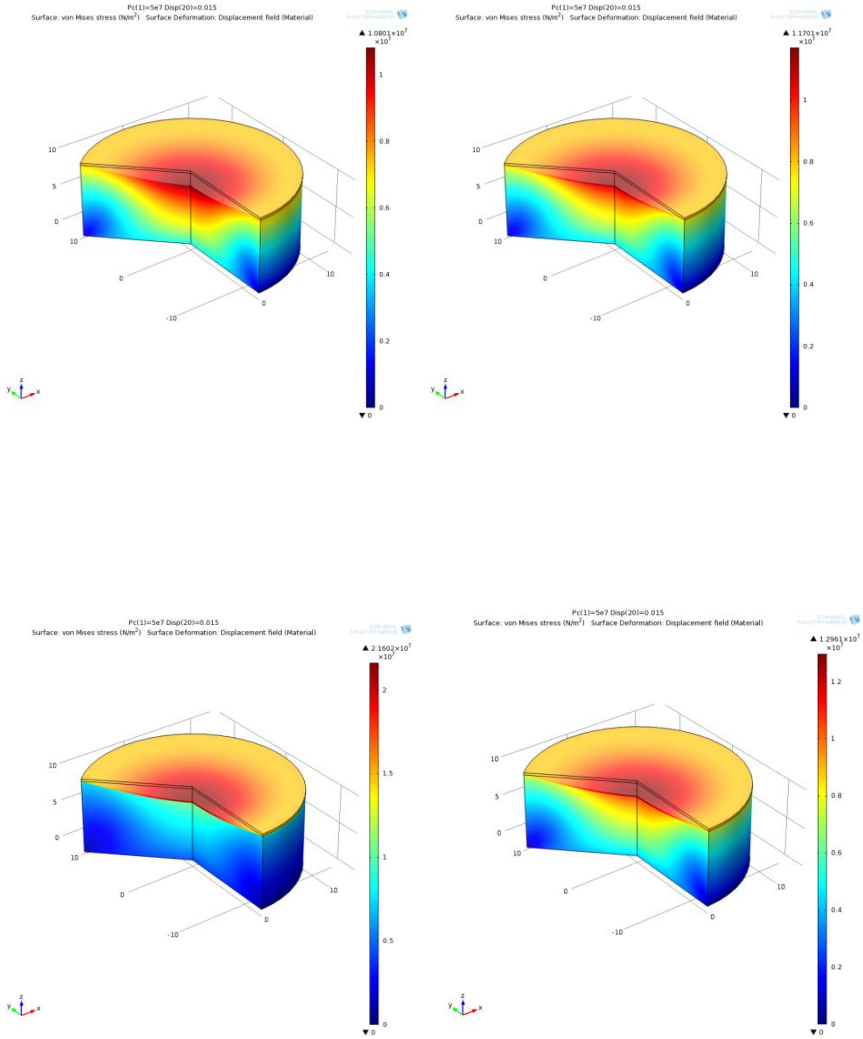

Figure 5.3 Criterion stress of compaction processed cell

Capter 6. Concluding remarks

6.1 Conclusion

We started this study to lower the operation temperature of SOFCs and reduce the process cost of SOFC unit cell. The attempt to fabricate YSZ/GDC bi-layered electrolyte cells via cold press process could prove great feasibility that a YSZ layer was able to enhance the performance and the durability of GDC-based SOFCs for intermediate temperature operation. And the cold press process can reduce some step of sintering process.

In summary,

- We deposited 50, 100, 200nm YSZ layer on bulk GDC via ALD successfully and confirmed them through FIB-SEM and XPS.

- We observed increases of over 50% in the peak power density and of about 5% in OCV at 600°C, and constant OCV over 8 hours under 5% hydrogen concentration with the 690 cycles (about 100nm) ALD-YSZ electrolyte cell unlike the case of the pure GDC case.

- With SEM results of reduced GDC and YSZ coated GDC, we could presume that the protective ALD-YSZ layer could prevent the ceria reduction which might result in electron conductivity and micro crackgeneration on GDC, so that it enabled enhanced ohmic resistance.

- We fabricated YSZ/GDC bi-layer electrolyte cell by cold press process which is simple and cost effective. We have obtained a higher 0.1V OCV, 15% higher power density of the cell from the cold press process than pure GDC cell at 600°C..

- In addition, we mixed PMMA and porous anode substrate material to make porous anode substrate. We obtained 630mW/cm^2 power density at 800°C. In order to improve of the electrochemical performance and the mechanical strength that is a disadvantage of porous anode substrate cell, we employed dense NiGDC anode functional layer by cold press process..

- We produced different thickness Anode functional layer cells. It was confirmed that optimal performance is obtained in the 20 micrometer thickness anode functional layer cell. It is recorded an OCV of 0.75V and power density of 911mW/cm^2 at 800 °C.

- Also, we were carried out numerical analysis about stress that is happened when undergo a cold press process, using the COMSOL multiphysics tool. It was confirmed stress criterion distribution according to the cell size of powder and overall cell dimestion size through the distribution of Sruface Von mise stress.

Whole test results are shown as Figure 6.1

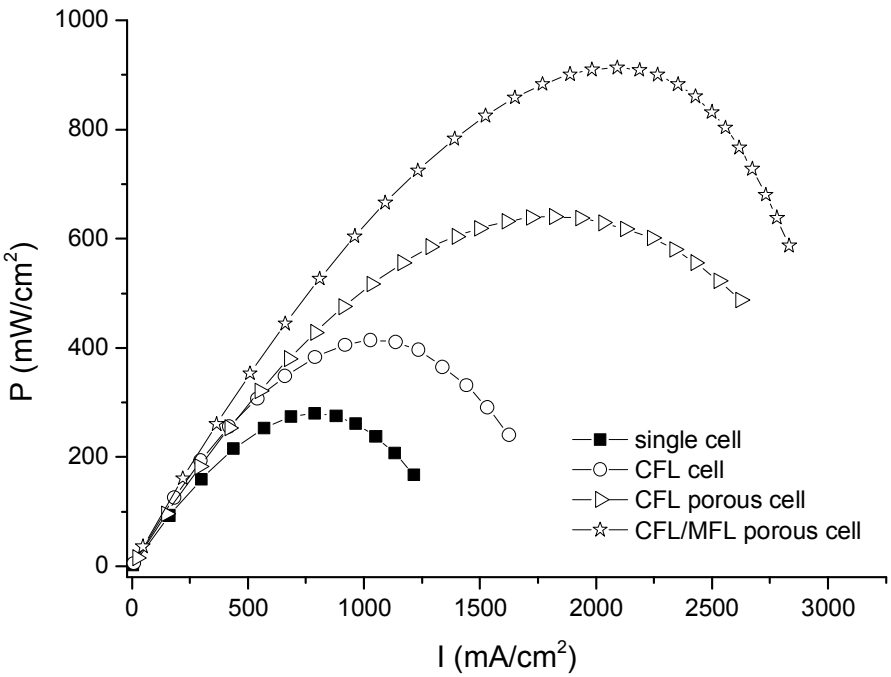

Figure 6. 1 Summary of whole test results in this study

6.2 Future works

More studies are necessary to reach the solution for this research. For example, we should find optimum YSZ/GDC thickness ratio. We also can examine optimum PMMA size for maximum power density.

Also, we have to find a way to lower sintering temperature. If we can control particle size of electrolyte powder and, find another adding material for lowering sintering temperature, we could achieve advantage in process and higher performance at identical conditions.

We need additional research in numerical analysis, too. We need coupled entire processing numerical analysis with compaction model and sintering model. We will provide directions which increase in the yield of the whole process by numerical analysis through the entire process.

Reference

1. CaSFCC, California Stationary Fuel Cell Collaborative, online: http://www.casfcc.org/2/StationaryFuelCells/FuelCellTechnologies.aspx

2. O'Hayre, R.P., et al., Fuel cell fundamentals. 2nd ed2009, Hoboken, NJ, USA: John Wiley & Sons.

3. Dicks, A. and J. Larminie, Fuel cell systems explained. 2nd ed2003, Hoboken, NJ, USA: SAE International and John Wiley & Sons.

4. 심준형, et al., 저온 작동 박막 고체산화물 연료전지. 한국세라믹학회지, 2006. 43(12): p. 751-757.

5. DOE, Types of fuel cells, online :

http://www1.eere.energy.gov/hydrogenandfuelcells/fuelcells/fc_types. html.

6. Singhal, S.C. and K. Kendall, High temperature solid oxide fuel cells: fundamentals, design, and applications. 1st ed2003, Amsterdam, Netherlands: Elsevier Science.

7. 손지원, et al., 박막공정의 융합화를 통한 초소형 고체산화물 연료전지의 제작: I. Spray Pyrolysis 법으로 증착된 Ni 기반 음극과 스퍼터링으로 증착된 YSZ 전해질의 다층구조. 한국세라믹학회지, 2007. 44(10): p. 589-595.

8. Garcia-Barriocanal, J., et al., Colossal ionic conductivity at interfaces of

epitaxial ZrO2:Y2O3/SrTiO3 heterostructures. Science, 2008. 321(5889): p. 676-680.

9. Ohring, M., The materials science of thin films. 2nd ed2002, Salt Lake City, UT, USA: Academic Press.

10. Beckel, D., et al., Thin films for micro solid oxide fuel cells. Journal of Power Sources, 2007. 173(1): p. 325-345.

11. LERMPS, Schematic representation of the magnetron sputterin process. (Zoom on the magnetron cathode), online:

http://lermps.utbm.fr/index.php?lang=en&pge=30

12. Mogensen, Mogens, Nigel M. Sammes, and Geoff A. Tompsett. "Physical, chemical and electrochemical properties of pure and doped ceria." Solid State Ionics 129.1 (2000): 63-94.

13. Aaltonen, T., Atomic layer deposition of noble metal thin films2005, Helsinki, Finland: University of Helsinki.

14. Kharton, V.V., F.M.B. Marques, and A. Atkinson, Transport properties of solid oxide electrolyte ceramics: a brief review. Solid State Ionics, 2004. 174(1): p. 135-149.

15. Yahiro, H., et al., High Temperature Fuel Cell with Ceria-Yttria Solid Electrolyte. Journal of the Electrochemical Society, 1988. 135(8): p.2077-2080.

16. Inoue, T., et al., Study of a solid oxide fuel cell with a ceria-based solid electrolyte. Solid State Ionics, 1989. 35(3-4): p. 285-291.

17. Eguchi, K., et al., Electrical properties of ceria-based oxides and their application to solid oxide fuel cells. Solid State Ionics, 1992. 52(1-3): p. 165-172.

18. Virkar, A.V., Theoretical analysis of solid oxide fuel cells with twolayer, composite electrolytes: electrolyte stability. Journal of the Electrochemical Society, 1991. 138(5): p. 1481-1487.

19. Mehta, K., R. Xu, and A.V. Virkar, Two-layer fuel cell electrolyte structure by sol-gel processing. Journal of Sol-Gel Science and Technology, 1998. 11(2): p. 203-207.

20. Chour, K.W., J. Chen, and R. Xu, Metal-organic vapor deposition of YSZ electrolyte layers for solid oxide fuel cell applications. Thin Solid Films, 1997. 304(1): p. 106-112.

21. Tsai, T., E. Perry, and S. Barnett, Low-temperature solid-oxide fuel cells utilizing thin bilayer electrolytes. Journal of the Electrochemical Society, 1997. 144(5): p. L130-L132.

22. Soral, P., U. Pal, and W.L. Worrell, Comparison of power densities and chemical potential variation in solid oxide fuel cells with multilayer and single-layer oxide electrolytes. Journal of the Electrochemical Society, 1998. 145(1): p. 99-106.

23. Wachsman, E.D., Functionally gradient bilayer oxide membranes and electrolytes. Solid State Ionics, 2002. 152: p. 657-662.

24. Park, J.Y. and E.D. Wachsman, Stable and high conductivity ceria/bismuth oxide bilayer electrolytes for lower temperature solid oxide fuel cells. Ionics, 2006. 12(1): p. 15-20.

25. Ahn, J.S., et al., High-performance bilayered electrolyte intermediate temperature solid oxide fuel cells. Electrochemistry Communications, 2009. 11(7): p. 1504-1507.

26. Chan, S.H., X.J. Chen, and K.A. Khor, A simple bilayer electrolyte model for solid oxide fuel cells. Solid State Ionics, 2003. 158(1): p. 29-43.

27. Liu, Q.L., et al., Anode-supported solid oxide fuel cell with yttriastabilized zirconia/gadolinia-doped ceria bilalyer electrolyte prepared by wet ceramic co-sintering process. Journal of Power Sources, 2006. 162(2): p. 1036-1042.

28. Bi, Z., et al., A high-performance anode-supported SOFC with LDCLSGM ilayer electrolytes. Electrochemical and Solid-State Letters,2004. 7(5): p. A105-A107.

29. Bi, Z., et al., Electrochemical evaluation of La0.6Sr0.4CoO3-La0.45Ce0.55O2 composite cathodes for anode-supported La0.45Ce0.55O2-La0.9Sr0.1Ga0.8Mg0.2O2.85 bilayer electrolyte solid oxide fuel cells. Solid State Ionics, 2005. 176(7-8): p. 655-661.

30. Zhang, X., et al., NiO–YSZ cermets supported low temperature solid oxide fuel cells. Journal of Power Sources, 2006. 161(1): p. 301-307.

31. Yang, D., et al., Low temperature solid oxide fuel cells with pulsed laser deposited bi-layer electrolyte. Journal of Power Sources, 2007. 164(1): p. 182-188.

32. Hui, S.R., et al., Metal-supported solid oxide fuel cell operated at 400–600°C. Journal of Power Sources, 2007. 167(2): p. 336-339.

33. Jang, W.S., S.H. Hyun, and S.G. Kim, Preparation of YSZ/YDC and YSZ/GDC

composite electrolytes by the tape casting and sol-gel dip drawing coating method for low-temperature SOFC. Journal of Materials Science, 2002. 37(12): p. 2535-2541.

34. Kim, S.G., et al., Fabrication and characterization of a YSZ/YDC composite electrolyte by a sol-gel coating method. Journal of Power Sources, 2002. 110(1): p. 222-228.

35. Wachsman, E.D., et al., Stable high conductivity ceria/bismuth oxide bilayered electrolytes. Journal of the Electrochemical Society, 1997. 144(1): p. 233-236.

36. Mehta, K., et al. Fabrication and characterization of YSZ-coated ceria electrolytes. in The Third International Symposium on Solid Oxide Fuel Cells. 1993. Honolulu: The Electrochemical Society.

37. Lim, H.T. and A.V. Virkar, Measurement of oxygen chemical potential in Gd2O3-doped ceria-Y2O3-stabilized zirconia bi-layer electrolyte, anode-supported solid oxide fuel cells. Journal of Power Sources, 2009. 192(2): p. 267-278.

38. Zhang, X., et al., Stability study of cermet-supported solid oxide fuel cells with bi-layered electrolyte. Journal of Power Sources, 2008. 185(2): p. 1049-1055.

39. Myung, D.H., et al., The effect of an ultra-thin zirconia blocking layer on the performance of a 1-μm-thick gadolinia-doped ceria electrolyte solid-oxide fuel cell. Journal of Power Sources, 2012. 206: p. 91-96.

40. Suzuki, T., et al., Fabrication and characterization of microtubular SOFCs with multilayered electrolyte. Electrochemical and Solid-State Letters, 2008. 11(6): p. B87-B90.

41. Leng, Y.J., S.H. Chan, and Q. Liu, Development of LSCF–GDC composite cathodes for low-temperature solid oxide fuel cells with thin film GDC electrolyte. International Journal of Hydrogen Energy, 2008. 33(14): p. 3808-3817.

42. Zha, S., W. Rauch, and M. Liu, Ni-Ce0.9Gd0.1O1.95 anode for GDC electrolyte-based low-temperature SOFCs. Solid State Ionics, 2004. 166(3): p. 241-250.

43. Zha, S., et al., GDC-based low-temperature SOFCs powered by hydrocarbon fuels. Journal of the Electrochemical Society, 2004. 151(8): p. A1128-A1133.

44. Zhen, Y.D., et al., Fabrication and performance of gadolinia-doped ceria-based intermediate-temperature solid oxide fuel cells. Journal of Power Sources, 2008. 178(1): p. 69-74.

45. Leng, Y.J., et al., Low-temperature SOFC with thin film GDC electrolyte prepared in situ by solid-state reaction. Solid State Ionics, 2004. 170(1): p. 9-15.

46. Xia, C. and M. Liu, Low-temperature SOFCs based on Gd0.1Ce0.9O1.95 fabricated by dry pressing. Solid State Ionics, 2001. 144(3): p. 249-255.

47. Liu, Q.L., K.A. Khor, and S.H. Chan, High-performance lowtemperature solid oxide fuel cell with novel BSCF cathode. Journal of Power Sources, 2006. 161(1): p. 123-128.

48. Yang, M., et al., Interaction of La0.8Sr0.2MnO3 interlayer with Gd0.1Ce0.9O1.95 electrolyte membrane and Ba0.5Sr0.5Co0.8Fe0.2O3−δ cathode in low-temperature solid oxide fuel cells. Journal of Power Sources, 2008. 185(2): p. 784-789.

49. Misono, T., et al., Ni-SDC cermet anode fabricated from NiO–SDC composite powder for intermediate temperature SOFC. Journal of Power Sources, 2006. 157(2): p. 754-757.

50. Joo, J.H. and G.M. Choi, Micro-solid oxide fuel cell using thick-film ceria. Solid State Ionics, 2009. 180(11-13): p. 839-842.

51. Kim, D.J., Lattice parameters, ionic conductivities, and solubility limits in fluorite-structure MO2 oxide [M= Hf4+, Zr4+, Ce4+, Th4+, U4+] solid solutions. Journal of the American Ceramic Society, 1989. 72(8): p. 1415-1421.

52. Bishop, S.R., K. Duncan, and E.D. Wachsman, Thermo-chemical expansion of SOFC materials. ECS Transactions, 2006. 1(7): p. 13-21.

53. Chiang, H.W., R.N. Blumenthal, and R.A. Fournelle, A high temperature lattice parameter and dilatometer study of the defect structure of nonstoichiometric cerium dioxide. Solid State Ionics, 1993. 66(1-2): p. 85-95.

54. Atkinson, A., Chemically-induced stresses in gadolinium-doped ceria solid oxide fuel cell electrolytes. Solid State Ionics, 1997. 95(3): p. 249-258.

55. 박상현, 전자 덫을 이용한 세리아계 전해질의 전해질 영역 제어, in 재료공학부 2008, 서울대학교 대학원: 서울.

56. Shim, J.H., et al., Atomic layer deposition of yttria-stabilized zirconia for solid oxide fuel cells. Chemistry of Materials, 2007. 19(15): p.3850-3854.

57. 권태현, 중온형 고체 산화물 연료전지용 이중층 전해질의 전 기화학

적 특성, in 재료공학부 2011, 서울대학교 대학원: 서울.

58. 하승범, Fabrication of nano-structured thin film solid oxide fuel cell by multi-deposition methods, in 기계항공공학부 2012, 서울대학교 대학원: 서울.

59. Moulder, J.F., et al., Handbook of x-ray photoelectron spectroscopy: a reference book of standard spectra for identification and interpretation of1992, Boca Raton, FL, USA: Perkin-Elmer. 261.

60. Matsui, T., et al., Electrochemical properties of ceria-based oxides for use in intermediate-temperature SOFCs. Solid State Ionics, 2005. 176(7): p. 647-654.

61. Yuan, S. and U. Pal, Analytic solution for charge transport and chemical-potential variation in single-layer and multilayer devices of different mixed-conducting oxides. Journal of the Electrochemical Society, 1996. 143(10): p. 3214-3222.

62. Zhang, X., et al., Internal shorting and fuel loss of a low temperature solid oxide fuel cell with SDC electrolyte. Journal of Power Sources, 2007. 164(2): p. 668-677.

63. Jung, H.Y., et al., Fabrication and performance evaluation of 3-cell SOFC stack based on planar 10cm×10cm anode-supported cells. Journal of Power Sources, 2006. 159(1): p. 478-483.

64. Tsoga, A., et al., Gadolinia-doped ceria and yttria stabilized zirconia interfaces: regarding their application for SOFC technology. Acta Materialia, 2000. 48(18-19): p. 4709-4714.

65. Zhou, X.D., B. Scarfino, and H.U. Anderson, Electrical conductivity and stability of Gd-doped ceria/Y-doped zirconia ceramics and thin films. Solid State Ionics, 2004. 175(1): p. 19-22.

66. Kwon, C.W., et al., High-performance micro-solid oxide fuel cells fabricated on nanoporous anodic aluminum oxide templates. Advanced Functional Materials, 2011. 21(6): p. 1154-1159.

67. Brahim, C., et al., Electrical properties of thin yttria-stabilized zirconia overlayers produced by atomic layer deposition for solid oxide fuel cell applications. Applied Surface Science, 2007. 253(8): p. 3962-3968.

68. Shim, J.H., et al., Intermediate-temperature ceramic fuel cells with thin film yttrium-doped barium zirconate electrolytes. Chemistry of Materials, 2009. 21(14): p. 3290-3296.

69. Huang, H., et al., High-performance ultrathin solid oxide fuel cells for low-temperature operation. Journal of the Electrochemical Society, 2007. 154(1): p. B20-B24.

70. Nguyen, Tuong Lan, et al. "Preparation and evaluation of doped ceria interlayer on supported stabilized zirconia electrolyte SOFCs by wet ceramic processes." Solid State Ionics 174.1 (2004): 163-174.

71. Kim, K. T., S. W. Choi, and H. Park. "Densification behavior of ceramic powder under cold compaction." Journal of engineering materials and technology 122.2 (2000): 238-244.

72. Chen, Peng, Gap-Yong Kim, and Jun Ni. "Investigations in the compaction and sintering of large ceramic parts." Journal of materials processing technology 190.1

(2007): 243-250.

73. Fan, Xiaofeng, et al. "Room Temperature Elastic Properties of Gadolinia-doped Ceria as a Function of Porosity." Ceramics International (2013).

74. Zhang, T. S., et al. "Preparation and mechanical properties of dense $Ce_{0.8}Gd_{0.2}O_{2-\delta}$ ceramics." Solid State Ionics 167.1 (2004): 191-196.

75. Ding, Changsheng, et al. "A simple, rapid spray method for preparing anode-supported solid oxide fuel cells with GDC electrolyte thin films." Journal of Membrane Science 350.1 (2010): 1-4.

76. Ding, Changsheng, et al. "Simple and rapid preparation of Ce< sub> 0.9</sub> Gd< sub> 0.1</sub> O< sub> 1.95</sub> electrolyte films for anode-supported solid oxide fuel cells." Surface and Coatings Technology 205.8 (2011): 2813-2817.

77. Chen, Peng, Gap-Yong Kim, and Jun Ni. "Investigations in the compaction and sintering of large ceramic parts." Journal of materials processing technology 190.1 (2007): 243-250.

78. Kim, K. T., S. W. Choi, and H. Park. "Densification behavior of ceramic powder under cold compaction." Journal of engineering materials and technology 122.2 (2000): 238-244.

79. Lee, S. C., and K. T. Kim. "Densification behavior of aluminum alloy powder under cold compaction." International journal of mechanical sciences 44.7 (2002): 1295-1308.

국문 초록

화석연료 고갈의 문제는 차치하고서라도, 경제적, 환경적, 지역적 문제들이 대두함에 따라, 앞으로 수소가 인류에게 있어서 마지막 자원 중에 하나가 되리라는 것은 우리에게는 이미 익숙한 사실이다. 이러한 수소를 이용하는 다양한 에너지 순환 시스템에 있어서 많은 연구자들이 연료전지를 차세대의 에너지 장치로 주목한 이래 다양한 상용화를 위한 연구가 진행 중이다.

통상적으로 고분자 연료전지는 빠른 동작시간, 충분한 전류밀도 등으로 인하여 차량용 전원 장치뿐만 아니라 발전용 전원으로도 많이 연구되고 있다. 하지만 물 관리 문제, 귀금속 촉매사용, 일산화 탄소 피독 등의 다양한 단점을 보이고 있는데 반해, 고체산화물 연료전지는 많은 장점을 가지고 있다.

이러한 고체산화물 연료전지의 상용화에 있어서도 많은 도전들이 있다. 그 중 가장 큰 문제점은 높은 작동온도에 있다. 높은 작동온도는 전극 전해질 구조의 열응력 문제, 니켈 응집, 구성물질간의 반응, 또 제한된 밀봉재의 선택문제, 그리고 고가의 분리판 물질 등의 다양한 문제를 발생시킨다. 또한 고분자 연료전지 등에 비하여 압축, 소결,, 그리고 각종 복잡한 고온 공정을 요구하기 때문에 공정에 있어서의 비용 문제도 상용화의 걸림돌 중 하나이다.

본 연구에서는 이러한 문제점을 해결하기 위하여 작동온도를 낮추고, 전해질의 두께를 줄이면서 기존의 방식에 비하여 공정의 수를 줄이고 시

간을 단축하여 비용을 줄이는 연구를 수행하였다.

우선 높은 이온 전도도를 가지는 가돌리니아 도핑 세리아(GDC) 상에 이트리아 안정화 지르코니아(YSZ) 를 증착한 이중층 전해질 고체산화물 연료전지 셀을 제작하여 중저온에서의 작동 및 성능과 내구성을 증대시키는 가능성을 확인하였다.

전자주사 현미경(SEM) 과 X 선 광전자 분광법(XPS) 을 통하여 성공적인 YSZ 증착을 확인하였고, 순수 GDC 전해질 셀과 달리 50% 이상의 출력 향상과 5% 높은 개회로 전압(OCV) 를 섭씨 600 도에서 얻을 수 있었다. 이는 YSZ 박막층이 GDC 의 환원을 막아주어 전압 강화와 저항 손실을 증가시키는 전자전도성과 미세균열을 방지한다는 것을 SEM 사진과 EIS 를 통하여 확인하였다.

둘째, 앞선 연구에서 GDC/YSZ 전해질 구조의 영향을 파악하였기 때문에, 더 높은 전력 밀도를 가질 수 있는 구조인 음극 지지체형 고체산화물 연료전지 셀에 이중층 구조를 적용하기 위한 연구를 진행하였다. 가소결한 음극 지지체에 습식법(wet ceramic process), 박막공정(thin film deposition) 등을 통한 다양한 접근을 시도하였고, 최종적으로 냉간압축법(Cold press process)으로 지지체에서 이중층까지 한 번에 소결하는 방법을 밝혀냈다.

냉간압축법의 단점인 층 두께 조절 및 균일도를 향상시키기 위해서 건조 스프레이코팅(dry spray coating) 으로 파우더를 적층하여 마이크로 단위의 두께를 컨트롤 하였다. 이렇게 하여 압축된 음극지지체-전

해질 이중층 셀을 동시 소결한 후에 스크린 프린팅(screen printing)을 이용하여 LSCF-GDC 양극을 제작하였다. 이러한 제작 방식은 습식법과 비교 하였을 때 한번 이상의 소결 공정을 줄일 수 있기 때문에 시간과 비용에서 큰 장점이 된다.

제작된 셀은 섭씨 600 도에서 210mW/cm^2 의 전력밀도를 달성하였고, 섭씨 800 도에서 최대 409mW/cm^2 의 전력밀도를 달성하였다. 이는 이중층 구조가 아닌 GDC 만을 이용한 실험과 비교 하였을 때, 개회로 전압은 0.1V, 최대 전력밀도는 15% 이상 향상된 결과이다.

셋째, 냉간압축법을 이용한 이중층 전해질 셀의 성능을 향상시키기 위한 제작 공정을 추가하였다. 앞선 이중층 전해질 셀의 음극지지체 분말에 PMMA 분말을 섞어주어 기공성을 향상시켜 제작한 결과 섭씨 700 도에서 460mW/cm^2 의 전력밀도를 달성하였다. 또한 기공성 음극지지체의 경우 생길 수 있는 기계적 강도의 약화를 보완하고, 전기화학적 성능을 향상시키기 위하여 음극지지체위에 기능층을 추가하여 냉간압축법으로 제작을 하였다. 그 결과 작동 시에도 안정적으로 기계적 강도가 유지되며, 더 향상된 전력밀도를 얻을 수 있었다.

마지막으로, 냉간압축법으로 제작 시에 발생하는 압축에 의한 셀의 파괴를 예측하기 위하여 COMSOL multiphysics 를 이용하여 응력계산을 진행하였다. 세라믹 파우더 압축 시 폰 마이즈 응력을 (von mise surface stress) Drucker-Prager Cap model 을 이용하여 예측하였다. 이러한 모델링을 통하여 압축 제작 시에 손상을 최소화 할 수 있는 분말의 조건 등을 확인할 수 있었다. 또한 앞으로 대면적 셀 제작을 위

한 기본적인 방향을 제시할 수 있었다.

주요어 : 고체산화물연료전지 (SOFC) 중저온, 가돌리니아 도핑 세리아 (GDC), 이중층 전해질, 음극지지체 구조, 냉간압축법 (Cold Press Process)

학번 : 2007-20864